UNIVERSITY OF SOUTHAMPTON

THE STRUCTURE OF POLYMER MELTS AND SOLIDS

Thesis submitted in respect of an application for the degree of

Master of Philosophy

E. R. SCERRI

March, 1979

DEDICATED TO MY MOTHER AND FATHER

ACKNOWLEDGEMENTS

I would like to thank Dr. P.J. Hendra for his supervision and guidance during this project,

also M.E.A. Cudby, Dr. H.A. Willis (I.C.I. Plastics Division) and P. Fydelor (Shrivenham Military College of Science) for the use of laboratory facilities and helpful discussions,

my colleagues Miss A. Castera, Dr. D.J. Cutler, Dr. M. Glotin and Dr. R.D. Sang,

the Science Research Council and I.C.I. for financial support.

CONTENTS

UNIVERSITY OF SOUTHAMPTON

ABSTRACT

FACULTY OF SCIENCE

CHEMISTRY

Master of Philosophy

THE STRUCTURE OF POLYMER MELTS AND SOLIDS

by Eric Robert Scerri

The thesis begins with a description of various models proposed to describe the structure of polymer melts and solids. This is followed by an experimental section with particular reference to Laser Raman spectroscopy and the use of the 'longitudinal acoustic mode' in characterising lamellar thicknesses in polymers.

Chapter III describes some experiments carried out by the author on polymers which were rapidly quenched from the melt. The findings show that theories based on polymer single crystals are inappropriate under these crystallisation conditions. This feature is of some industrial importance as the large scale manufacture of polymers likewise involves rapid cooling from the molten state.

Experimental data obtained on irradiated polyethylene is presented and suggests that chain entanglements influence the crystallisation behaviour of polymers.

The final chapter extends the range of rapid cooling experiments in order to investigate quenching from below the melting point. The behaviour thus observed suggests an analogy with that of rubber and a possible explanation for the variation of lamellar thickness with temperature as described throughout this report.

CHAPTER I INTRODUCTION: THE STRUCTURE OF POLYMER MELTS AND SOLIDS

The structure of polymer melts and solids produced from them is at present a highly controversial field of study. A large number of experimental techniques have been employed and numerous models of the structures have been proposed.

The Ordered Melt.

The relatively high densities of molten polymers is taken by some authors as an indication of a high degree of chain order. Robertson showed that the high densities (shown in Table 1) could be explained by an almost parallel alignment of chain segments (1).

From the ratio of the crystalline to amorphous densities an angle of divergence θ between the chains is calculated and found to have a value of 15^{o} in polyethylene. This value of θ is used to compute a radius of gyration for polyethylene of $1.56 \times 10^{-7} M^{\frac{1}{2}}$ cm. This is approximately 15 times the value obtained experimentally (2) and the inconsistency is explained by assuming that the polymer chain can fold back on itself.

Table 1.1 A comparison of amorphous and crystalline densities of several polymers.

Polymer	Crystalline density dc	Amorphous density da	$\frac{da}{dc}$	θ	Reference
Polyethylene	1.00	0.855	0.855	15^{o}	(3)
Polypropylene	0.937	0.854	0.911	8.4	(4)
Isotactic Polystyrene	1.111	1.054	0.947	4.8	(4)
Polyvinyl Alcohol	1.345	1.269	0.943	5.2	(5)
Nylon 66 (α)	1.220	1.069	0.876	12.4	(6)

Some of the earliest work carried out on the structure of molten polymers was that of Kargin. From an analysis of electron diffraction patterns he deduced that parallel chain molecules were present in molten polyethylene (7). Some recent investigations however show no evidence of this form and attribute the conclusions of Kargin to an inaccurate interpretation of data (8). A peak which had originally been assigned to an intermolecular distance of 5 Angstroms was found to correspond to a distribution of distances when a correction for background scattering had been suitably performed.

A structural model of the melt phase proposed by Yeh is based on the appearance of a nodule-like structure of 20-50 Angstroms in diameter in glasses quenched from polymer melts (9). These features resemble spherulites found in melt crystallised materials and as in the case of spherulites they are thought to indicate the presence of ordered chain packing.

This two-phase structural model shown in figure 1.1 is referred to as the folded chain micellar model and is also supported by electron diffraction and microscopic studies of amorphous polymers (10).

Figure 1.1 Folded chain micellar model of molten polymers (10).

The appearance of a nodular structure has also been suggested by electron microscopy studies made by Schoon (11).

Harget and Siegmann have observed density differences associated with nodular and internodular regions by means of small angle X-ray diffraction (12). Recent investigations however maintain that no density differences exist in polymers other than those due to random thermal fluctuations. It is also argued that a nodular structure does not necessarily imply the presence of ordered chains since these nodules have also been observed in inorganic glasses where chain parallelism cannot exist (8). Other authors using X-ray and electron diffraction methods have reported that polymers tend to show one diffuse ring in addition to rings due to intramolecular spacings. They attributed the diffuse ring to the average spacing between parallel neighbouring chain segments (13).

Based on the observations of density and the scattering experiments on molten polyethylene which have been mentioned, Pechhold has developed a structural model which accounts for an intermolecular potential arising from parallel chains (14). This approach begins with

an ideal crystal and introduces defects such as kinks and folds in order to obtain an overall isotropic melt. From theoretical considerations of the interactions between different types of pairs of chains in different geometrical arrangements, various properties of polyethylene are calculated and found to agree with experiment to a high degree of accuracy. These properties include the melting point and the change of melting point and volume as a function of static pressure. By proposing the "meandering" of whole bundles of molecules the model is extended to account for the overall isotropy of molten polymers while retaining local order in the form of parallel chains. A meander radius of fifty Angstroms is estimated for polyethylene and this quantity is linked with the observations of Yeh and Schoon (9, 11). The meander curvature is shown to be kinetically hindered from crystallising and thus yields the amorphous phase of the two phase model observed spectroscopically on crystallised polymers. The fold length is predicted to be approximately 200 Angstroms which agrees reasonably well with the lamellar thickness observed by Raman spectroscopy on the crystalline solids produced by cooling from the melt.

Figure 1.2 Meander model of polymer melts introduced by Pechhold (14)

The disordered melt.

Light scattering experiments on molten polymers suggest the presence of a random arrangement of chains. From a knowledge of the intensity of scattered light as a function of scattering angle and by assuming a random structure, the radii of gyration of various polymer solutions have been derived (15). The random coil model on which these calculations are based maintains that no intermolecular forces exist between polymer chains. The effect of volume exclusion which occurs as a result of the self intersection of polymer chains is compensated for by extrapolation of the scattering data to the so called " θ point" (16).

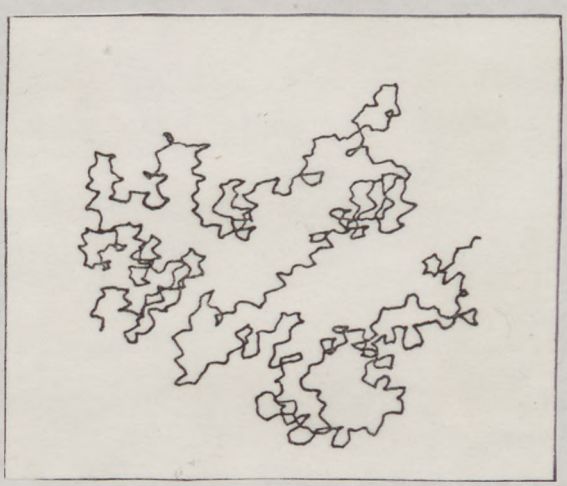

Figure 1.3 Random coil model of molten polymers.

Recently these values of radius of gyration values have been independently confirmed by means of neutron scattering studies. For example polyethylene of molecular weight 80,000 has a radius of gyration of 123 $\pm$ 5 Angstroms on the random coil model while neutron scattering experiments yielded a value of 12.5 $\pm$ 3 Angstroms (8).

In the latter technique a contrast between neutron scattering factors is provided by using a mixture of perdeuterated and protonated polymer

molecules. A small percentage of normal polymer is mixed into a matrix of deuterated polymer or vice versa. Although the overall structure appears to be one of random coil from these experiments, it has been pointed out that the existence of local order on a scale of about 30 Angstroms is not precluded (8).

Crystallisation of Polymers.

One of the first models developed to describe the structure of solid polyethylene was the fringed micelle (17, 18).

Small crystals or micelles were envisaged as being molecularly interconnected by the polymer chains. The model shown in figure 1.4 incorporated both short sections of chain parallelism and regions of amorphous polymer. In this way the fact that the density and melting points observed in polyethylene were not those expected of a fully crystalline material could be accounted for. Furthermore the X-ray diffraction pattern revealed the broadening of the two principal peaks and therefore the presence of some amorphous material.

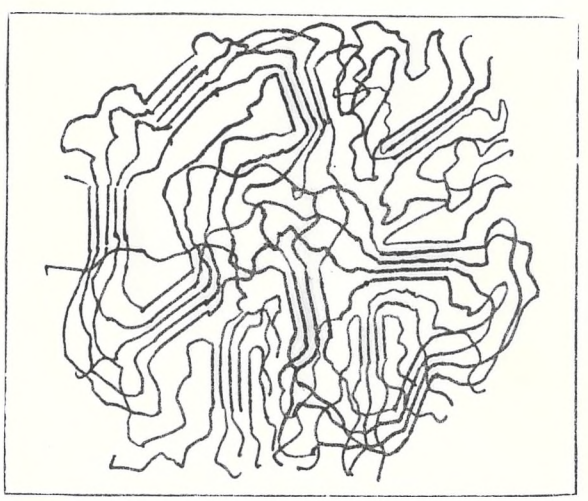

Figure 1.4 Diagram of fringed micelle.

From 1945 onwards a feature known as spherulites became recognised in crystallised polyethylene which could not be readily explained on the basis of the fringed micelle model (19, 20). These features often circular in shape displayed the property of binefringence when viewed under a polarising microscope. It was deduced that the polymer had a considerable anisotropy or a high proportion of molecular ordering in order to produce such a difference in refractive index along perpendicular directions. The spherulites appear as a Maltese Cross pattern which produces interference effects as the analyser of the microscope is rotated. In some cases concentric rings are seen superimposed on the image of the spherulite.

Sometime later highly crystalline polymers began to appear and to be investigated. They resulted from the use of Ziegler catalysts which produce polymers of high steric regularity. These polymers displayed spherulites more clearly and made possible the preparation of single crystals of many polymers. These single crystals were almost simultaneously obtained in various laboratories by crystalisation from dilute solution of polyethylene in xylene (21 - 23). Examination of the material prepared in this way revealed the existence of thin platelet or "lamellar" crystals.

These crystals were found to be of roughly 100 Angstroms thickness and displaying well defined crystallorgraphic facets. Electron diffraction studies confirmed the single-crystal nature of the lamellae and showed that the chain orientation was either perpendicular or at a large angle to the basal surface of the crystal. A chain folded model illustrated in figure 1.5 was developed to include all these features and explain how a chain many times longer than the layer thickness could be confined within the lamellae. The fold length was envisaged as being fairly uniform so as to give rise to the smooth surface observed by electron microscopy.

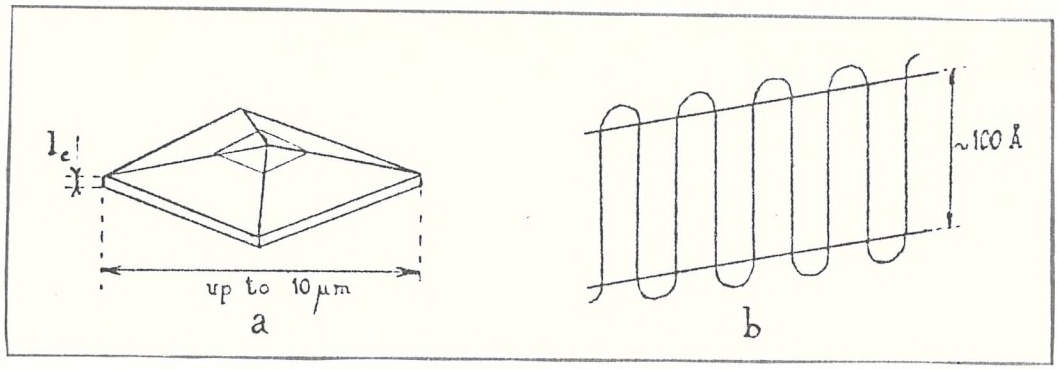

Figure 1.5 (a) lamellar crystal (schematic representation)
(b) chain orientation in a lamellar crystal.

Various other polymers including polypropylene (24), some polyethers (25) polyamides (26) and polyesters (27) have also been crystallised from solution and the lamellar crystals thus formed have been described by the chain folding model. Complex biological molecules such as polypeptides and D.N.A. can also be obtained in a chain folded form (28).

Soon after the chain folded model had been applied to solution grown crystals of polyethylene it became apparent that the same explanation might apply to melt crystallised polyethylene.

The fold length or straight chain segment gives rise to low angle X-ray diffraction effects. The identification of lamellae has proved to be more difficult in the case of melt crystallised material in which these entities are less accessible to observation than in single crystals. The procedure usually adopted has been to establish certain features from solution crystallisation and to apply this knowledge to crystallisation from the melt (29 -32). Several techniques however, such as low angle X-ray diffraction, electron microscopy, Raman spectroscopy and oxidation followed by G.P.C. analysis have repeatedly demonstrated the existence of lamellae (33).

Among the earliest evidence which suggested that chain folded lamellae were common to both single crystals and melt crystallised material was the observation of the annealing phenomenon in both types of samples. If the polymer is held at a temperature just below the

melting point an increase occurs in the lamellar thickness. Keller and O'Connor first observed this behaviour in polyethylene single crystals (34). In order to explain this behaviour Reneker has suggested the movement of defects along the chains up to the fold surface where the extra material is ejected to make the lamella thicker (35). The defect is envisaged as a twist in the chain as shown in figure 1.6

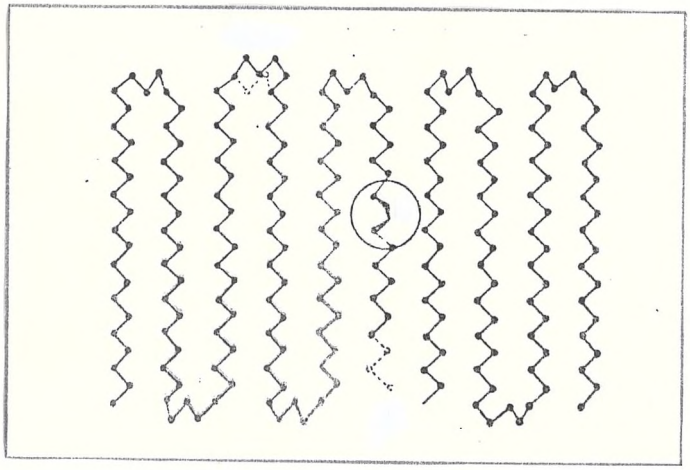

Figure 1.6 Representation of the annealing mechanism proposed by Reneker (35).

This model envisages the chains threading through the lamellae and pulling the chain ends with them. Keller and Priest have contested this aspect by showing that the concentration of chain ends on the surfaces of polyethylene lamellae does not change appreciably during annealing (36). An alternative annealing mechanism has been proposed in which the chains rearrange locally and produce thickening of lamellae in integral numbers of the original fold lengths (37). This was first noticed in polyamides (38) and later in the initial stages of annealing in polyethylene.

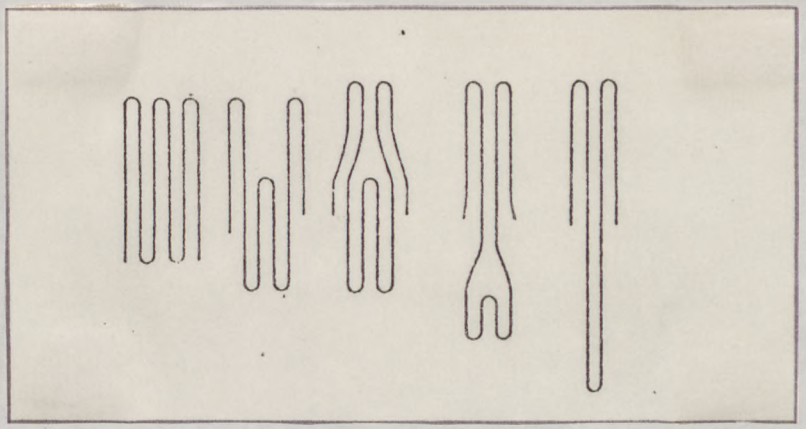

Figure 1.7 A chain refolding scheme leading to a twofold increase in lamellar thickness (Keller and Dreyfuss).

The mechanism shown in figure 1.7 implies the presence of defects as in Reneker's model but in the former case the defects are due to folds buried within the crystal interior. In the melt crystallised polymers, annealing occurs at a slower rate than in single crystal material and the precise mechanism involved is not well understood at present.

The spherulites which are features of melt crystallised samples as has already been mentioned are also believed to incorporate folded polymer chains. The chain folding is thought to occur at right angles to the radial direction of the spherulite. The so called spherulite fibrils consisting of lamellar units are found twisting around the radial direction and thus give rise to the observed pattern of concentric rings, as seen in figure 1.8.

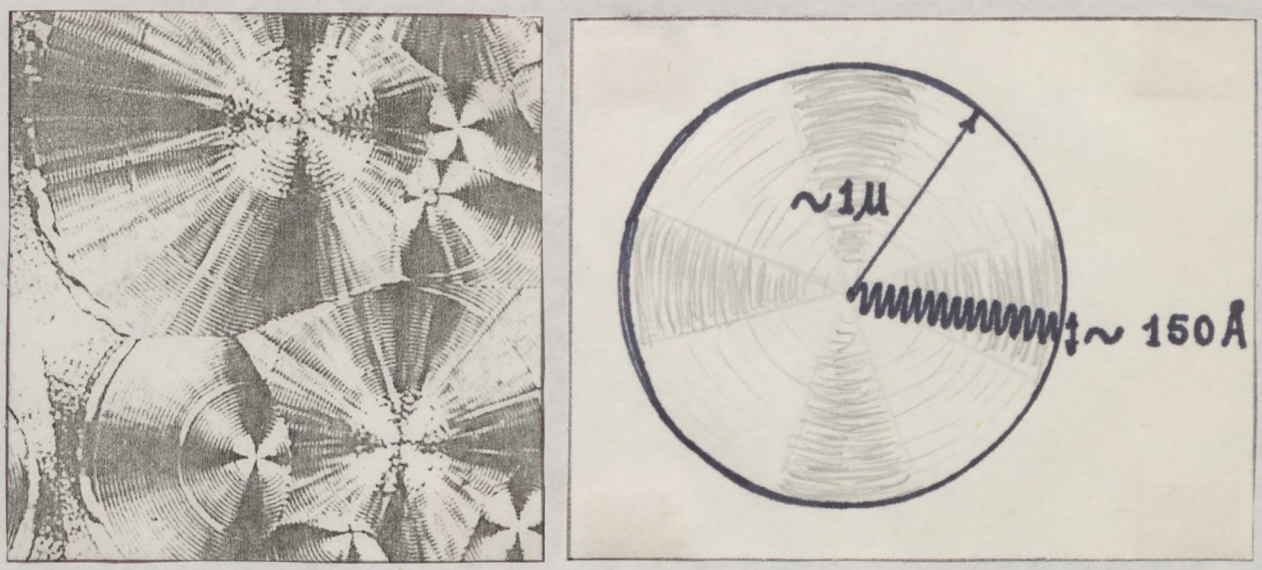

Figure 1.8 Photograph of polymer spherulites (39) and typical dimensions in polyethylene spherulites (right).

The nature of the folds has been a much debated question since the introduction of the chain folding concept. Various models illustrated in figure 1.9 have been proposed and they include sharp folds, loose loops with adjacent (40) or non-adjacent re-entry(41), the "switchboard model" (42) and a composite model (43).

The smooth lamellar surface observed microscopically suggests the presence of sharp folds. Support for the loose loop model is provided by the work of Cobbold and Palmer (44). Chain segments from the fold surface were removed by etching with nitric acid and were found to have a narrow distribution in length of about eleven carbon atoms. This is considerably larger than a tight fold which calculations have shown to comprise of five carbon atoms (45).

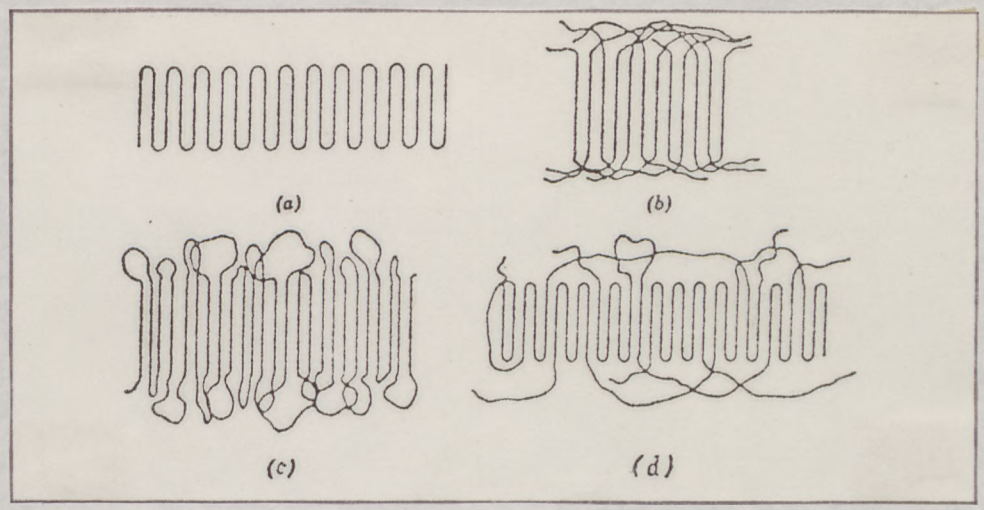

Figure 1.9 Two dimensional representation of models of the fold surface in polymer lamellae. (a) sharp folds, (b) loose loops with adjacent re-entry, (c) switchboard model, (d) a composite model.

Theories of polymer crystallisation and their experimental verification.

Various theories have been developed to describe the crystallisation of polymers. They aim to explain why chain folding occurs and to predict the dependence of the fold length on crystallisation temperature and supercooling.

The theories were originally based on solution crystallised materials and subsequently applied or extended to the case of melt crystallisation. The first theories which were proposed fall under the category of thermodynamic theories. They are based on the consideration of producing a fold length which is the most thermodynamically stable, i.e. corresponding to a minimum free energy of the system (46), (47). The folding of chains is not necessarily required by this approach but it is one way in which the crystal size can be limited to a particular value. The thermodynamic theories suffer from not accounting for the exact relation between fold length and supercooling. It was realised in the early 1960's that although thermodynamic factors

might contribute to the fold length a deeper insight into the problem would be gained from a kinetic approach. This theory is based on classical nucleation theory with an emphasis on the secondary nucleation process. The core thickness can be altered during the growth of a crystal by changing the crystallisation temperature thus indicating that the governing factors do not lie in the initial formation of the crystal or primary nucleation. According to kinetic theories the observed fold length corresponds to the structure with maximum crystallisation rate rather than maximum thermodynamic stability.

Each of the kinetic theories is based on a simple model of a new chain which is deposited along an existing crystal face (48-51). The pre-existing thickness of substrate face is of no importance and experiments have also shown that the fold length is determined by the prevailing supercooling (52).

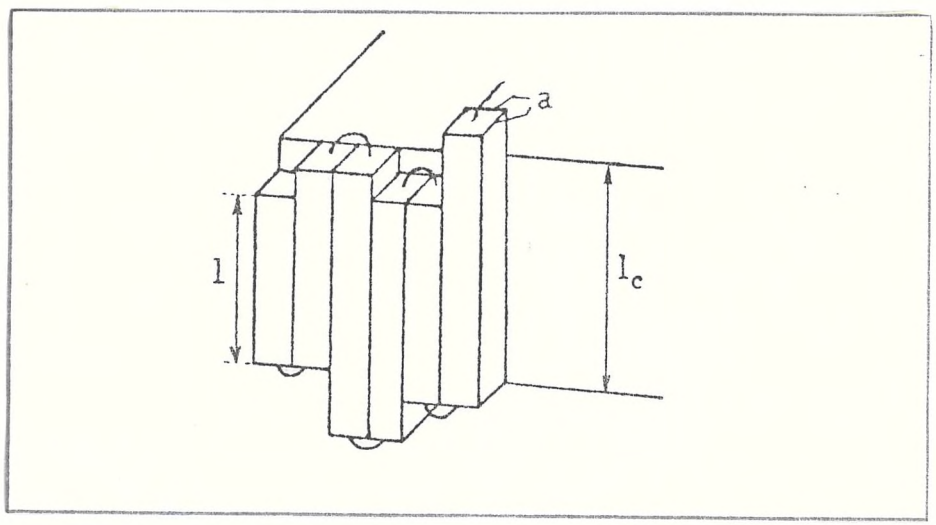

Figure 1.10 Representation of the deposition of a new crystalline layer on a pre-existing nucleus.

The models consider two competing effects as the chain folds. Deposition of a new chain segment causes a reduction in free energy of the system. The deposition also creates two new surfaces and consequently a compensating increase in the free energy. These two opposing trends

produce a fold length at which the deposition rate is maximised and the various theories differ somewhat in the calculation of this most probable fold length. All the theories provide the same general expression for the fold length L*

$$L^* = \frac{2\,\sigma_e\,T_m}{\Delta H \Delta T} + \delta L$$

Where Tm is the melting temperature of the fully extended chain crystal

ΔH is the heat of fusion

ΔT is the supercooling (Tm - Tc) where Tc is the crystallisation temperature.

σ_e is the surface free energy of the basal plane of the crystal

δL differs according to each theory and represents about 15% of the first term at all except extreme supercoolings.

In the theory of Lauritzen and Hoffman the second term on the left hand side of the equation is given by

$$\frac{kT}{a\sigma_s}$$

where k is Boltzmann's constant

a the dimension of the base of a chain segment

σ_s the surface free energy of the side of a chain segment.

More sophisticated theories have allowed for the possibility that the fold length may vary in the deposition process and it was concluded that crystallisation can only occur below a certain supercooling. Lauritzen and Passaglia have given a treatment in which they estimate the surface roughness of lamellar crystals to be of the order of 8 - 14 Angstroms (51). It should be added that many of these theories have claimed agreement with experiment as a result of the large uncertainties in the values of T_m^o and therefore ΔT, σ_s, and σ_e. The approach due to Hoffman and Lauritzen was specifically applied to crystallisation from

the melt and the conclusion reached was that primary nucleation involves folded chain nuclei (48). These authors furthermore maintined that a truly amorphous state of polyethylene could not be obtained under any cooling conditions.

Although the supercooling dependence of the fold length has been demonstrated in single crystals, this cannot be said of melt crystallised materials. Polyethylene which is very rapidly cooled from the melt has been found to display a lamellar thickness which is independent of the supercooling but is a function of the melt temperature (53). This Raman spectroscopic evidence suggests that chain folding is not predominant in melt crystallised polyethylene. This present report provides further evidence of this form for the case of polyoxymethylene (54). Similar conclusions have been reached from neutron scattering experiments on solid polymers. The root mean squared radius of gyration of polymers in the melt state and the solid state are found to be similar and to vary with molecular weight. The molecular organisation in the melt is therefore thought to be the same as that in the solid. As in the neutron scattering studies on the melt state the contrast arises from the different scattering powers of perdeuterated and protonated polymers. The examination of most solid polymers by this technique suffers however from a serious drawback and particularly so in polyethylene. The melting points of the protonated and deuterated forms of polyethylene differ by $6^{o}C$, As a result there is a tendency for segregation to occur as the mixture is cooled (55), (56). Ballard et. al. have tried to reduce the segregation problem by using branched chain protonated polyethylene together with linear deuterated material so that the crystallisation temperatures would match. This method was successful in eliminating clustering in rapidly quenched samples. In similar experiments with slowly crystallised samples however, the measured molecular weights were many times the true value thus indicating some segregation between the two types of polymer molecules. (57). The results obtained on quenched

samples indicate a high degree of disorder which is incompatible with the chain folded model. Further evidence against chain folding is provided by the work of several authors on the radial growth of spherulites as a function of supercooling in polyethylene (58, 59). It was found that the rate of deposition along the growing lamellae is about 10^5 - 10^6 sequences per second.

Measurements of relaxation rate of polyethylene show tnat this is far too slow to occur during the development of the crystal front (60). The completion of the relaxation process would be essential for the deposition of the molecule in a regularly folded structure.

A new model was introduced in the early 1960's in order to describe the structure of melt crystallised polymers (61-63). This model has more recently become known as the "solidifaction model". The polymer chains are seen to traverse crystalline regions and then either to re-enter the same lamella or to enter the adjacent lamellae. The re-entry of chains to adjacent sites (i.e. regular chain folding) is considered to be a rare event in this model shown in figure 1.11

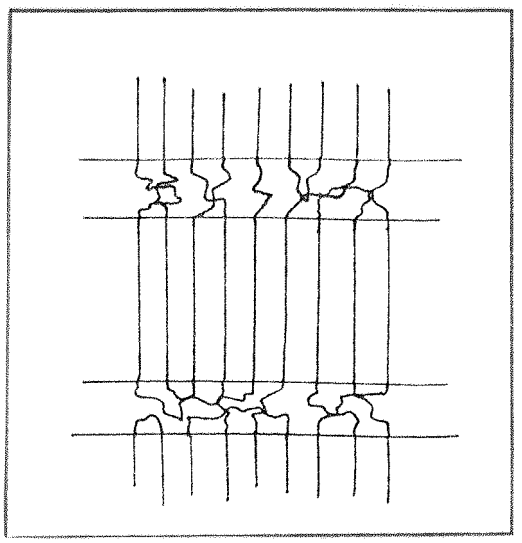

Figure 1.11 The solidification model of polymer crystallisation.

The model furthermore suggests that neighbouring lamellae are to a large degree interconnected by the entanglement of chains in the amorphous region. This present report offers some evidence for the existence of entanglements and their influence on the crystallisation of polyethylene.

CHAPTER II EXPERIMENTAL TECHNIQUES

Molecular vibrations, infra-red and Raman activity.

By considering the symmetry of molecular vibrations it is possible to obtain a knowledge of their infra-red and Raman activity. For example, the carbon dioxide molecule has four fundamental vibrations as shown in figure 2.1.

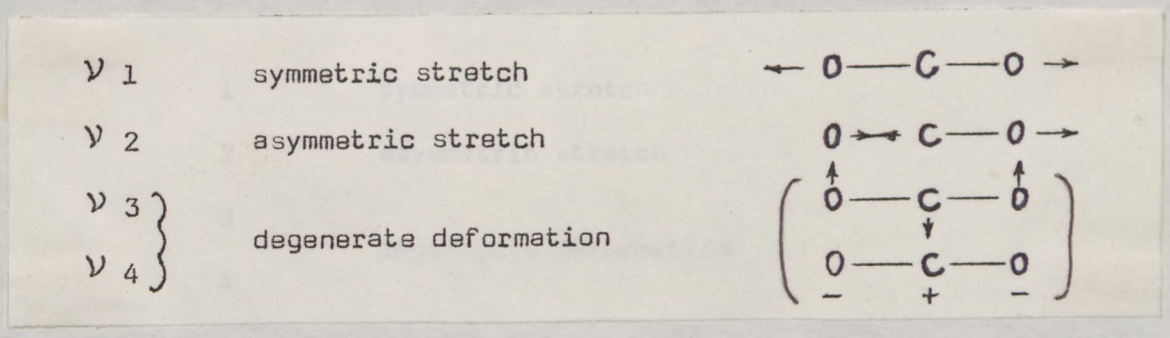

Figure 2.1 Fundamental vibrations of the carbon dioxide molecule.

During the course of the symmetric stretching vibration no change occurs in the dipole moment of the molecule. This fact renders the mode infra-red inactive. Raman activity depends upon the periodic fluctuation of the polarisability of the molecule. More precisely, the variation of the polarisability in respect of the progress of the vibration must possess a non-zero gradient at the equilibrium position.

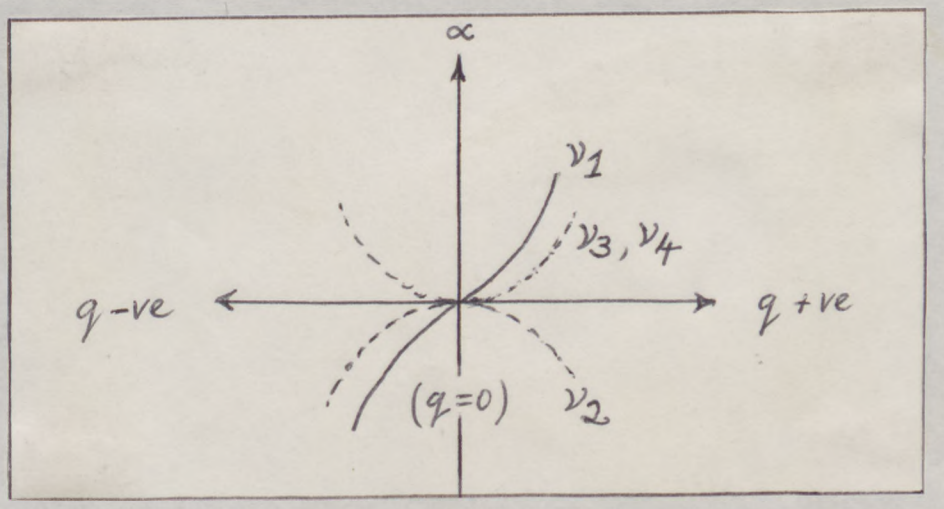

Figure 2.2 Polarisability as a function of bond extension in the vibrational modes of carbon dioxide.

Polarisability is a measure of the ease with which electrons may be induced to flow under a stimulus, and this property varies with the deformation or extension of bonds.

The symmetric vibration does cause a difference in bond extension and from a plot of the polarisability α against the desplacement co-ordinate q it can be seen that at q = 0 the change in polarisability has a non-zero gradient. This mode is therefore Raman active.

The three other vibrational modes also produce changes in polarisability, but their curves all snow zero gradient at the equilibrium positions and are consequently inactive to the Raman effect. Their dipole moments undergo a reversal in direction in the course of the bond deformation, thus rendering them infra-red active.

In molecules possessing a centre of symmetry such as the example considered, the mutual exclusion principle is applicable and states that no vibrational mode shall give rise to both infra-red and Raman transitions. In less symmetrical molecules this rule can be broken and some modes show both types of transition.

In the case of polymers a further complication arises in that although the monomer unit may be centrosymmetric such as in polyethylene, the "coincidence" of spectral bands nevertheless occurs as a result of chain defects or folding.

Another peculiar feature of polymer spectroscopy if the apparent lack of observed bands.

The number of independent normal modes of vibration is given by 3N - 5 in the case of a linear molecule and 3N - 6 for a non-linear molecule, where N is the number of atoms. A normal mode represents a periodic contortion of the molecule occuring in such a way that all the atoms traverse the equilibrium configuration together. For polyethylene of molecular weight 50,000 the value of N is approximately 12,000 from which a possible 36,000 normal modes are expected. In practice however a few classes of vibrations appear to have almost identical frequencies, thus greatly simplifying the spectrum. This

feature is illustrated in the form of a density of states plot in

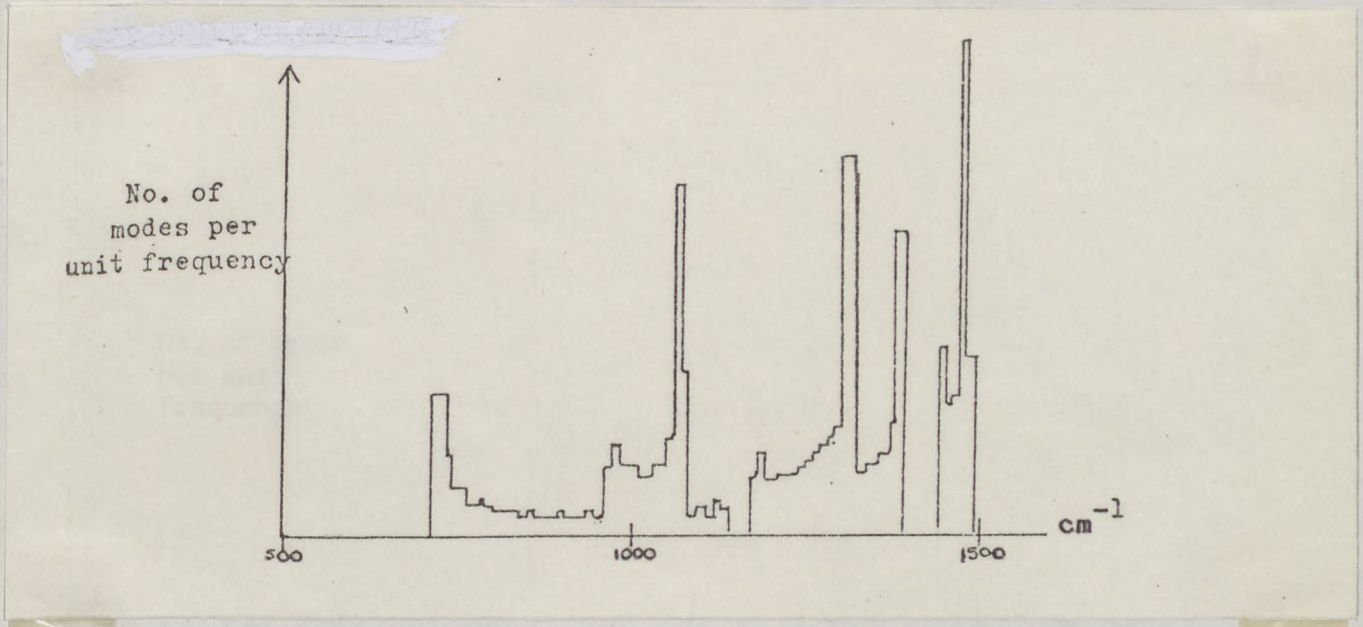

Figure 2.3 Density of states for a trans polyethylene chain (64)

This property arises because a change in the phase relationship between neighbouring CH_2 groups generally gives rise to a small change in the frequency of vibration.

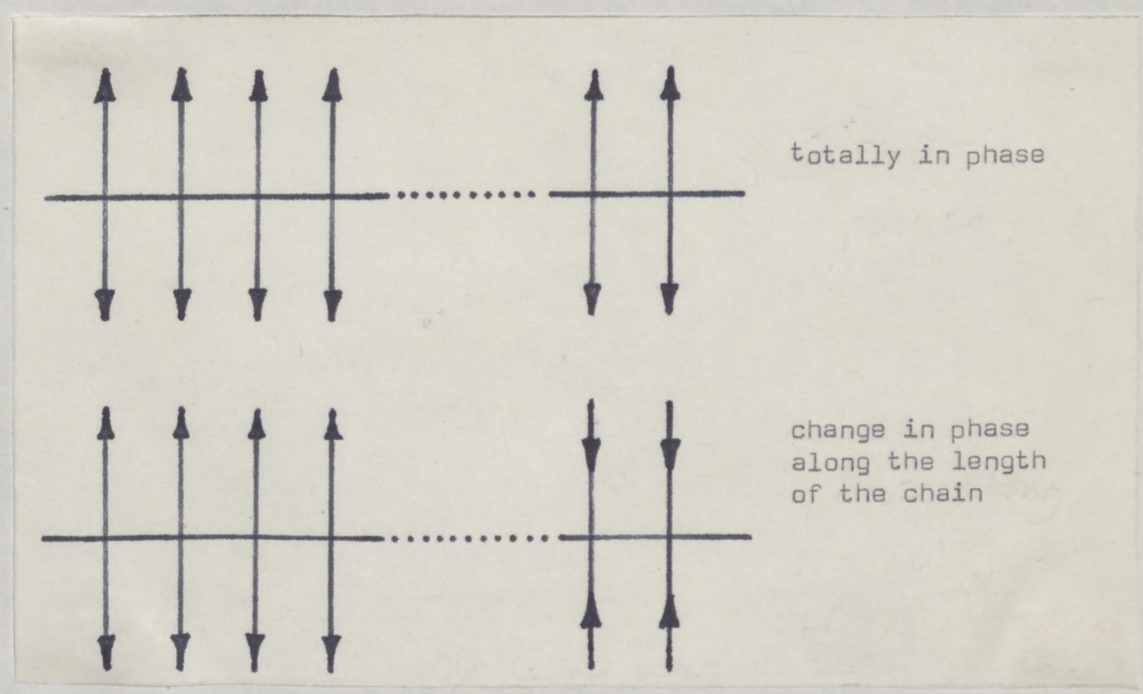

Figure 2.4 Phase change in the stretching mode of polyethylene.

For each mode the effect of this form of phase shift on the frequency may be plotted on a dispersion curve.

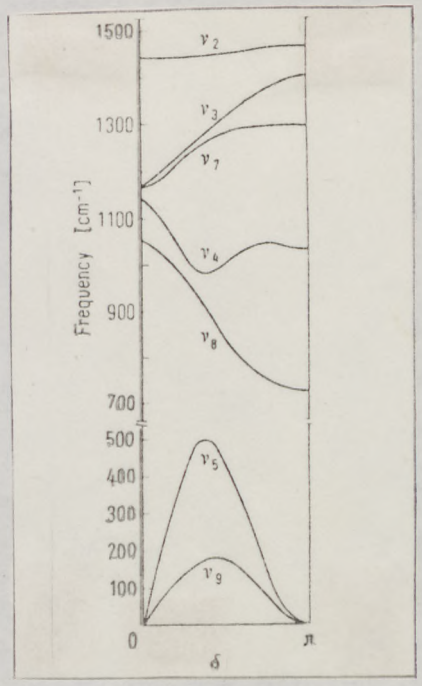

Figure 2.5 Dispersion curve of polyethylene.

In the case of an infinite or very long polymer chains the only active vibrations are those for which $\delta = 0$ and $\delta \neq \pi$. Shorter chains such as those of paraffin molecules are not restricted in this way and the so called band progression effect may be observed corresponding to several phase relationships between neighbouring CH_2 groups (65). The vibrational modes which appear in the phase dispersion curve fall broadly into three categories of acoustic or low energy modes, lattice modes and internal modes in order of increasing energy. This thesis is especially concerned with the acoustic modes of polymers, particularly the longitudinal modes.

The spectra of polymer can also be simplified as for any type of molecule, by the application of group theory to classify the vibrations according to symmetry classes. The C_2H_4 molecule is representative of polyethylene and its symmetry elements transform as do the elements of the D_2h point group. By using the character table of the D_2h point group

The symmetry classes of all the possible vibrations may be predicted. It is also possible to predict the number of active vibrations belonging to each symmetry class (66).

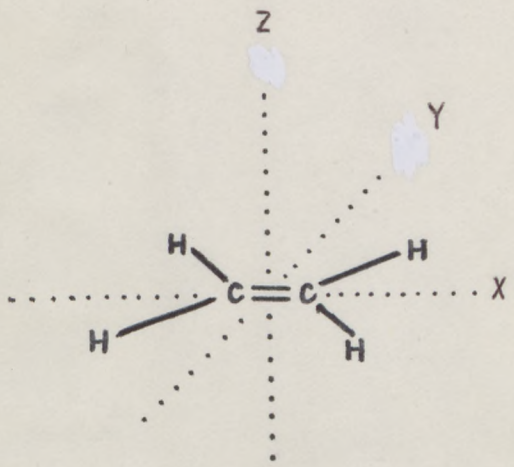

Symmetry properties:
3 x 2 fold axes along X, Y AND Z (C_2)
Centre of Symmetry (i)
3 x reflection planes in XY, YZ and XZ planes (66)

D_2h point group.

Figure 2.6 The symmetry of the ethylene molecule.

Table 2.1 The character table of the D_2h point group (67).

D_{2h}	E	$C_2(z)$	$C_2(y)$	$C_2(x)$	i	$\sigma_h(xy)$	$\sigma_h(xz)$	$\sigma_h(yz)$		
A_{1g}	1	1	1	1	1	1	1	1	x^2, y^2, z^2	
A_{1u}	1	1	1	1	−1	−1	−1	−1		
B_{1g}	1	1	−1	−1	1	1	−1	−1	xy	R_z
B_{1u}	1	1	−1	−1	−1	−1	1	1	z	
B_{2g}	1	−1	1	−1	1	−1	1	−1	xz	R_y
B_{2u}	1	−1	1	−1	−1	1	−1	1	y	
B_{3g}	1	−1	−1	1	1	−1	−1	1	yz	R_x
B_{3u}	1	−1	−1	1	−1	1	1	−1	x	

The Raman spectroscopy experiment.

A dipole moment is induced in a sample by means of a beam of electro-magnetic radiation. In the case of a laser beam of frequency ν_0 the induced dipole **P** is given by the expression:

$$P = \alpha E = \alpha E_0 \cos (2\pi \nu_0 t)$$

where α = polarisability of the sample

E = electric vector of incident radiation

E_0 = amplitude of the wave expressed as a vector

ν_0 = frequency of the incident laser radiation

t = time

The induced dipole radiates energy, the effect being known as Rayleigh scattering.

As a result of molecular vibrations and corresponding changes in polarisability the above relation is more generally expressed as:

$$P = 2\alpha E_0(\cos 2\pi \nu_0 t) + E_0 q_0 \frac{\partial \alpha}{\partial q}\left[\cos 2\pi(\nu_0 + \nu_{vib})t + \cos 2\pi(\nu_0 - \nu_{vib})t\right]$$

with q as the vibrational coordinate and ν_{vib} the frequency of vibration. The scattering which occurs at the frequencies $(\nu_0 \pm \nu_{vib})$ is termed inelastic and constitutes the Raman effect. The $(\nu_0 - \nu_{vib})$ inelastic contribution, is the more intense of the inelastic terms and consequently spectra are recorded by scanning from the laser frequency to smaller frequencies.

The measurement of lamellar thickness.

Several methods are currently used for the investigation of lamellae in polymers:-

(1) Low-angle X-ray diffraction (L.A.X.D.)

(2) Electron microscopy of fracture surfaces. The lamellar thickness can be measured directly from the shadow length in electron micrographs. Techniques (1) and (2) are often used in conjunction

with one another.

(3) Chemical methods such as the oxidation destruction of chain folds at the lamellar surface followed by analysis of the molecular fragments by G.L.C.

(4) Vibrational spectroscopy. A measure of lamellar thickness is obtained from the Raman active longitudinal acoustic mode in polymers.

The first three of these techniques are more established, but the use of vibrational spectroscopy is presently attracting a great deal of interest because of the relative ease with which the lamellar thickness may be derived. In this present study the Raman spectroscopic method has been employed and in some instances supporting information is provided by L.A.X.D. studies. In the former technique the molecular vibrations under investigation are those of the whole chain molecules. The frequency of vibration of the chain is proportional to the reciprocal length of the chain and this feature is exploited in the study of polymeric materials. In 1941, Mizushima et. al. first observed that in a series of solid n-paraffins the frequencies of the Raman active bonds were independant of the number of carbon atoms with the exception of the band of lowest frequency (68). This band was assigned to the first order accordion-like vibration and is known as the longitudinal acoustic mode or L.A. mode. The atoms within the carbon chain vibrate in the direction of the chain axis.

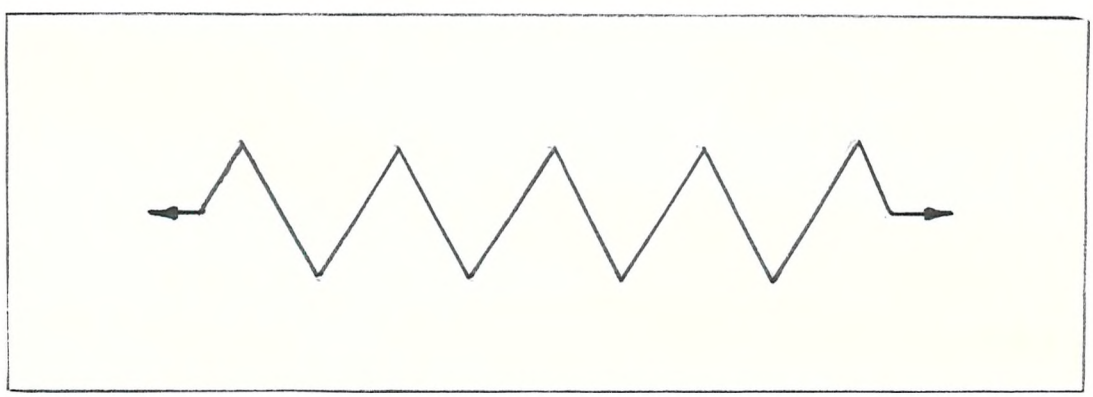

Figure 2.7 Representation of the first order L.A. mode.

Figure 2.7 represents the first order L.A. mode in which the frequency of vibration ν and the vibrating length l are related by the following expression:

$$\nu = \frac{m}{2lc}\left[\frac{E}{\rho}\right]^{\frac{1}{2}}$$

where E is the Young's modulus of the chain axis

ρ is the crystalline density

c is the velocity of light

m is the mode order

The correlation between lamellar thickness as assessed by techniques (1 - 4) is of primary importance and is currently the subject of active discussion. Early results showed a good correlation between Raman derived chain length and X-ray long spacing (69). The simplest interpretation of the spectroscopically derived lamellar thickness is one in which the chain is terminated by gauche units in the fold regions at each end.

On this simple picture the Raman measurement gives a measure of the crystalline core while the X-ray data reflects the overall layer thickness.

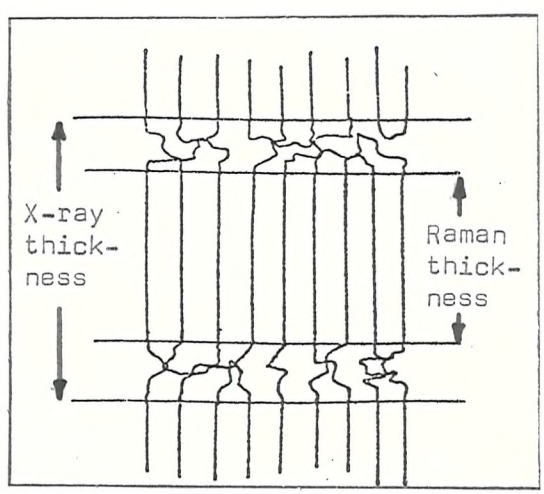

Figure 2.8 Measurement of lamellar thickness by Raman and X-ray techniques.

The Raman derived length are generally smaller than the X-ray long spacing, but instances have been reported where as a result of chain tilting the Raman length is found to be the greater of the two parameters (70,71)

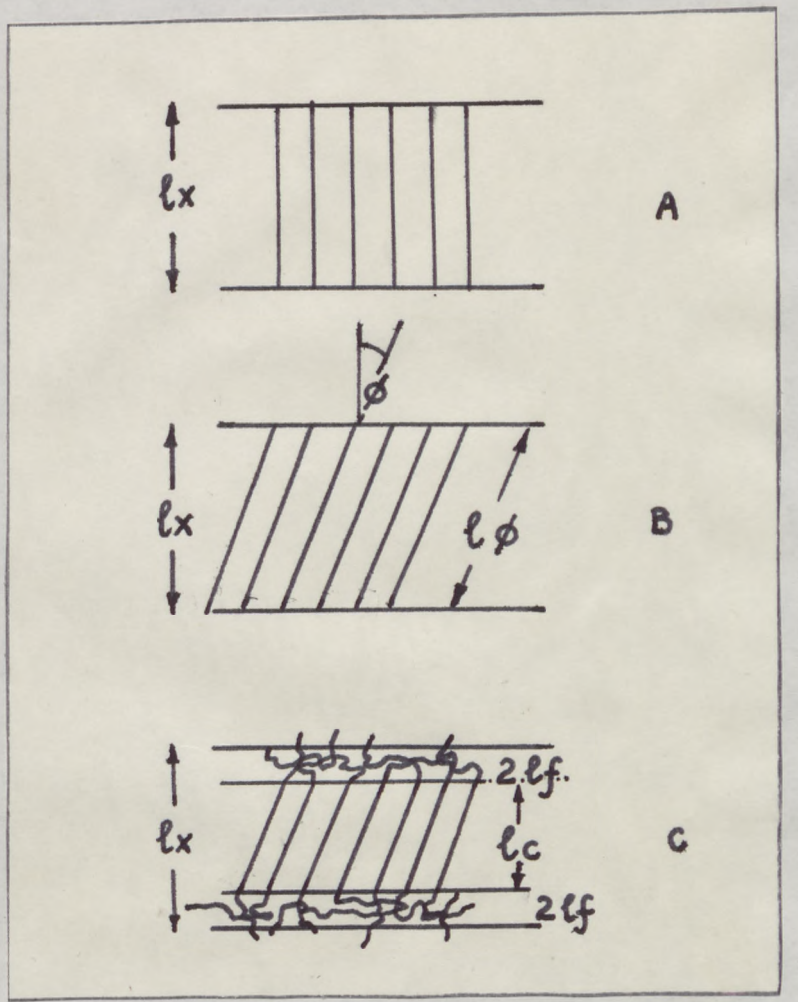

Figure 2.9 Lamellar crystals with identical layer thickness parallel to lamellar normal lx, but with different morphologies (72)

a Paraffin with no chain tilt.
b Paraffin chains tilted at angle of ø.
c Polyethylene lamellae with chain tilt and amorphous regions.

The interpretation that L.A. mode provides a measure of the crystalline core thickness free from perturbations from the fold phase has been a source of controversy among researchers. Olf et. al. undertook a detailed study in which they found that annealing of polyethylene caused no significant change in the L.A. mode frequency. They also showed that the swelling samples of the polymer in xylene also had no effect on the frequency of the L.A. mode. In both these experiments it is thought that changes occur in the amorphous portion of the polymer and that if this phase were also involved in the acoustic vibration then changes would occur in the observed spectral frequency (69). Nevertheless these authors considered that some other experimental data obtained on the relative intensities of the higher order was sufficiently important to outweigh the above findings and to indicate that the amorphous phase is indeed involved in the vibration. This evidence which had been available for some time showed that whereas n-paraffin molecules possessed a series of easily resolvable higher order modes (n = 1 to about n = 15) in the case of polyethylene it was only possible to obtain the n = 1,3,5 bands. The authors rationalised these differences by proposing a composite rod model in which both the crystalline and amorphous phases contributed to produce a single L.A. mode frequency and its higher order modes.

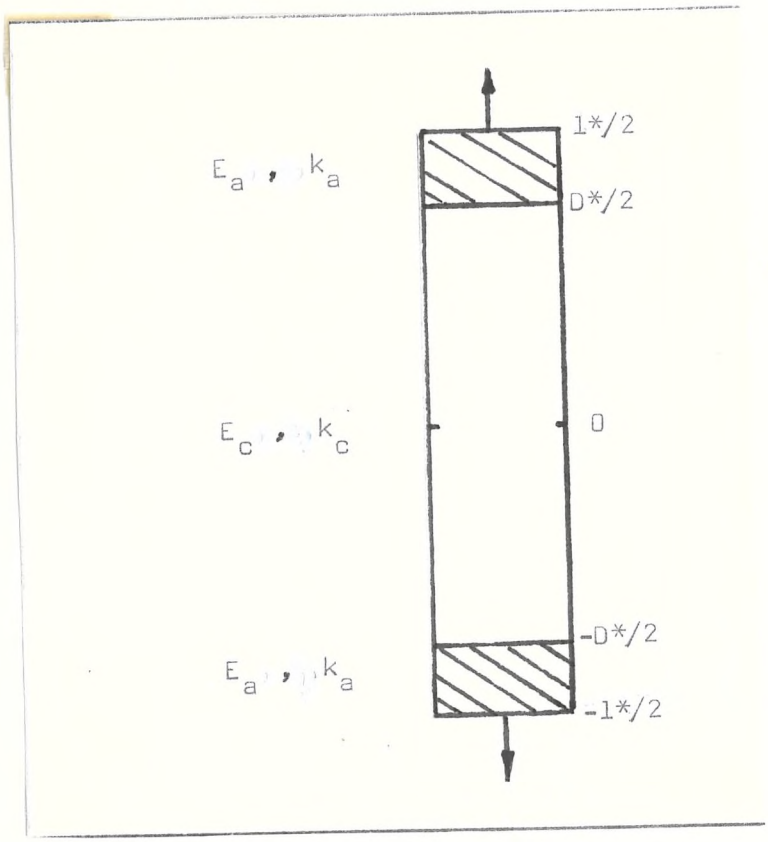

Figure 2.10 Composite rod model of the polyethylene L.A. mode.

A mathematical analysis of the problem shows that for this composite rod the equation determining its natural frequency to be the following:

$$k_c E_c \cot k_c D^*/2 = k_a E_a \tan k_a 1^*/2$$

where k_c = propagation constant in the crystalline core

k_a = propagation constant in the amorphous region

E_c = Young's modulus in the crystalline core

E_a = Young's modulus in the amorphous region

$D^*/2$= the length of half the crystalline core

$1^*/2$= the length of half the total amorphous content.

This treatment has the effect of reducing the intensities of higher order mode frequencies in polyethylene so that they agree approximately with the observed intensities. In the case of n-paraffins the usual expression for L.A. mode frequency remains applicable as the amorphous content is negligible.

An alternative approach which does not involve an amorphous phase contribution to the L.A. mode has been examined by Fraser in connection with the problem of higher order mode frequencies (73). It is pointed out that the population of energy levels contributes significantly to the observed spectroscopic intensities. If the observed intensities are multiplied by a Boltzmann distribution term of

$$(1 - \exp(-h\bar{\nu}c / kT))^{-1}$$

then the intensities are found to obey a dependence on $\frac{1}{m}$ where m is the L.A. mode order. By an appropriate substitution, the above correction term is found to increase by a factor of 30 times in the region between 1 cm^{-1} and 30 cm^{-1} where the L.A. mode of polyethyle is normally observed. Paraffin molecules have L.A. modes at higher frequencies of between 30 cm^{-1} and 500 cm^{-1} where the correction term increases by a factor of about 7. The frequency dependence of the population of energy levels is thus shown to explain the apparent differences between paraffins and polyethylene and furthermore that surface fold effects peculiar to polyethylene need not be invoked. The effect of the distribution of lamellar thickness of the intensity and width of the L.A. mode has been investigated theoretically (74). It is predicted that for a sample with a Gaussian distribution of lamellar thicknesses the relative lowering of the intensity and the width of the L.A. mode are defined by a factor S.

$$S = \frac{\text{mean lamellar thickness}}{\text{standard deviation of lamellar thickness distribution.}}$$

The influence of methyl group branches on the L.A. mode in alkanes and polyethylene was investigated by Fanconi and Crissman (75). They recorded the Raman spectra of n - $C_{20}H_{42}$ and two of its isomers; 2-methyl nonadecane and 10 methyl nonadecane. In this way a knowledge

was obtained of how the presence of methyl branching and the position of the methyl group affected the frequency of the L.A. mode. The isomer with a methyl group branch at the end of an all-trans chain was found to lower the fundamental L.A. mode frequency to that of an all-trans chain one carbon atom longer. The higher overtones of the L.A. mode showed a larger shift of approximately 10 cm^{-1} for n = 5. This behaviour suggests that a distribution of branch methyl groups in polyethylene lamellae would give rise to a broad frequency distribution in the higher order modes in agreement with the experimental findings. A methyl branch near the centre of the chain was found to have no effect on the L.A. mode in the isomer of n-C_{20}-H_{42}. It was also noted that in both of the isomers of n-C_{20}-H_{42} the presence of the extra mass due to the methyl branch did not disrupt the longitudinal acoustic mode.

A lowering of the L.A. mode frequency by end groups has also been observed for fatty acids (76).

Srobl and Eckel have carried out a detailed analysis of the relative positions of the L.A. modes in n-paraffins and polyethylene (77). Their belief is that inter lamellar forces contribute to the observed L.A. modes and that they affect the relative positions of the higher order modes even in the case of n-paraffins. For example in $C_{94}H_{180}$ some deviations are present from a frequency ratio of

$$\nu_1 : \nu_3 : \nu_5 = 1:3:5$$

as given by the general expression (see page 25).

By accounting for the inter lamellar forces they obtain the following corrections to the frequencies:

$$\nu_1 = \nu f + \Delta\nu$$

$$\nu_3 = 3\nu f + \Delta\nu/3$$

$$\nu_5 = 5\nu f + \Delta\nu/5$$

The observed frequencies show a remarkable agreement with these formulae and can be represented as:

$$\nu_1\ (cm^{-1}) = 24.2 + 2.2 = 26.4$$

$$\nu_3\ (cm^{-1}) = 72.6 + 0.7 = 73.3$$

$$\nu_5\ (cm^{-1}) = 121.0 + 0.5 = 121.5$$

In the case of separated or uncoupled lamellae the fundamental frequency would lie at 24.2 cm^{-1} and the interlamellar force leads to a shift of 2.2 cm^{-1}.

A variety of methods have been used to etch lamellae in order to remove the amorphous material. (78, 79, 80). One such study was carried out by subjecting polyethylene samples to fuming nitric acid at 60°C for a period of 4 days. The L.A. mode of several samples were found to have identical values before and after the removal of the amorphous phase from which it was inferred that the L.A. mode is solely governed by the vibration of the crystalline core (80). This form of treatment is known to introduce carboxy and nitro groups in place of the amorphous material, but these entities appear not to affect the frequency of the L.A. mode (81).

An extensive study of the effect of swelling the amorphous regions with various polymers showed that the L.A. mode was very little affected, (82), whereas the X-ray long spacing has previously been shown to change considerably following the degradation treatment (83).
It may be concluded from these various studies that the L.A. mode in polyethylene does give a reliable measure of the crystalline core thickness although end groups and methyl branching may give rise to small changes.

In the case of helical polymers however, most authors appear to favour an amorphous contribution to the L.A. mode (84, 85, 86). Hartley et. al. observed the fundamental (ν_1) L.A. mode and the third harmonic (ν_3) in molecular weight fractions of polyethyl oxide. Their findings

of the relative frequencies of these transitions were explained by means of the composite rod model of Olf and co-workers (70). A perfectly crystalline rod would show a value of 3 for the ratio of ν_3/ν_1 whereas the samples examined gave the values shown in Table 2.2.

Table 2.2 L.A. modes in polyethylene oxide molecular weight fractions (84).

Approximate M_n	ν_1	ν_3/ν_1
1500	12.5	1.6
2000	9.2	2.1
4000	7.8	2.4
20000	7.0	2.6

Rabolt and Fanconi carried out a series of annealing experiments on polyoxymethylene and found a strong correlation between small-angle scattering maxima and the frequency of the L.A. mode (86). A plot of the Raman frequency versus the reciprocal of the measured X-ray long period gave a straight line passing through the origin as is characteristic of longitudinal acoustic modes. By assuming that the spectral transition is associated with the crystalline core and taking the crystalline density of P.O.M. to be 1.491 g/cm^3 they calculated a value of 18.9 x 10^{11} Pa for the Young's modulus. The X-ray method, whereby the change in lattice constant is measured as a function of applied stress yields a significantly smaller value of Ec = 5.4 x 10^{11}Pa (87). Calculations by Piseri and Zerbi have provided a value of Ec = 15.3 x 10^{11}Pa (88), while neutron scattering experiments on single crystals of polyoxymethylene yield Ec = 15.0 x 10^{11}Pa (89). In view of the discrepancy between these values it is not at present possible to derive absolute

values of lamellar thickness from the L.A. mode frequencies observed in polyoxymethylene. It is however felt by the author that the L.A. mode provides a useful measure of lamellar thickness on the basis of the good correlation with X-ray data and also the relative ease with which the Raman measurements may be carried out. Similarly in polyethylene the Raman method provides a simple and rapid technique for measuring the lamellar thickness without any special sample requirements. The low angle X-ray technique however employs fairly large samples which are free from voids and of uniform thickness. All the lamellar thickness values presented in this study were derived from the L.A. mode frequency and in some cases also from L.A.X.D. data.

Laser Raman spectrometer and related techniques.

Spectra were recorded on a Coderg T800 Raman spectrometer using the green light of an argon ion laser (5145 Angstroms) as a source of illumination. Dispersion of the scattered radiation is provided by a triple monochromator system and the radiation leaving the monochromators is detected by a photomultiplier tube (90). Figure 2.11 shows the optical diagram of the Coderg spectrometer. The electron pulses produced are "sorted" to remove noise pulses from those due to the optical signal and attenuated to energies of a constant value. A rectifier is used to produce a d.c. voltage (proportional to the number of photons per second arriving at the photomultiplier tube) which is displayed on a chart recorder. Solid samples are mounted on a small clamp on the table of the spectrometer and illuminated with a finely focused laser beam so that the scattered radiation enters the collection lens of the spectrometer. The reduction in the diameter of the laser beam produces an increase in illumination. The reduced beam is typically focused to a diameter of a few microns by means of a suitable lens

(see figure 2.13), and the use of a small volume of illumination facilitates the collection of scattered radiation over a wide angle. A sample optics system in which the viewing direction is at 90^{o} to the illumination at the sample is employed in the spectrometer. The instrument is also provided with Vernier adjustments to allow accurate alignment of the sample. The errors occuring in recording the L.A. mode are due to the width of the band, the signal to noise ratio, the background scattering and the apparent variation of the exciting line frequency. The last of these problems is usually overcome by plotting the exciting line frequency before each L.A. mode is recorded. However this procedure requires interrupting the scan and changing the size of the slits to avoid damaging the photomultiplier tube. Results obtained by this method are quoted with an error of $\pm$ 0.5 cm^{-1}. In more accurate studies several sheets of paper were placed in front of the collecting lens thus making it possible to scan through the exciting line. The sheets of paper were then simply removed while the scan was continuing and the L.A. mode was recorded as usual. The distance between the two peaks could then be measured to give a direct measure of the L.A. mode with an accuracy of approximately $\pm$ 0.1 cm^{-1}. A correction was made to the observed L.A. mode in order to account for the steeply rising Gaussian background due to elastic scattering by samples. This procedure was carried out on a Dupont A310 curve resolver where both the L.A. mode and the Rayleigh (elastic scattering peak) were approximated by Gaussian curves. The elastic scattering was subtracted and the resulting change in the position of the L.A. mode (usually between 0.5 and 1.5 cm^{-1}) was noted. The L.A. mode of a polyethylene sample was recorded on five occassions and it was found that the corrected values obtained by this more accurate technique were reliable to $\pm$ 0.25 cm^{-1}.

A glass cell shown in figure 2.15 was used to record Raman spectra at low temperatures. Samples were mounted on the tip of a "cold finger" which was maintained at the temperature of liquid nitrogen (boiling point 77K).

Infra-red spectroscopy.

A Perkin-Elmer 580 ratio recording spectrometer at the Plastics Division of I.C.I. was used to monitor changes in unsaturation in radiation crosslinked samples of polyethylene. In this instrument the ratio of the energy in the sample and reference beams is continuously measured thus providing greater sensitivity than in a null balance spectrometer. In the latter type of instrument the transmission of the sample is observed for half the time of the operation cycle. The signal operates a servo mechanism which drives a comb along the comparison beam until the energy passing along the two paths is the same. The comb comes to rest at this point because there is no out-of-balance signal. The comb is geared directly to a pen recorder to obtain a trace of the percentage of light transmitted by the sample. In the true ratio recording instrument a comb is not required. The two beams are separated after amplification, rectified and fed to a potentiometer recorder. The reference beam potential is applied to the whole slide wire and the signal potential to the variable contact.

Polymer samples are most conveniently observed by infra-red spectroscopy if they are in the form of thin films. A small hydraulic press fitted with 6 in. square platens and with provision for heating these platens to 350^{o}C was used to prepared such films of typically 100 μ thickness. The powdered or granule form of polymer was pressed between polished stainless steel plates having been sandwiched between two sheets of aluminium foil to facilitate stripping of the pressed film.

Quenching of the samples was carried out by circulating water through the platens or by rapidly transferring the polymer together with the steel plates into a container of liquid nitrogen.

Optical microscopy.

The examination of polymer spherulites was carried out between the crossed polars of an optical microscope. The instrument used in this study was a Vickers A10 photographic microscope with X400 magnification.

X-ray diffraction.

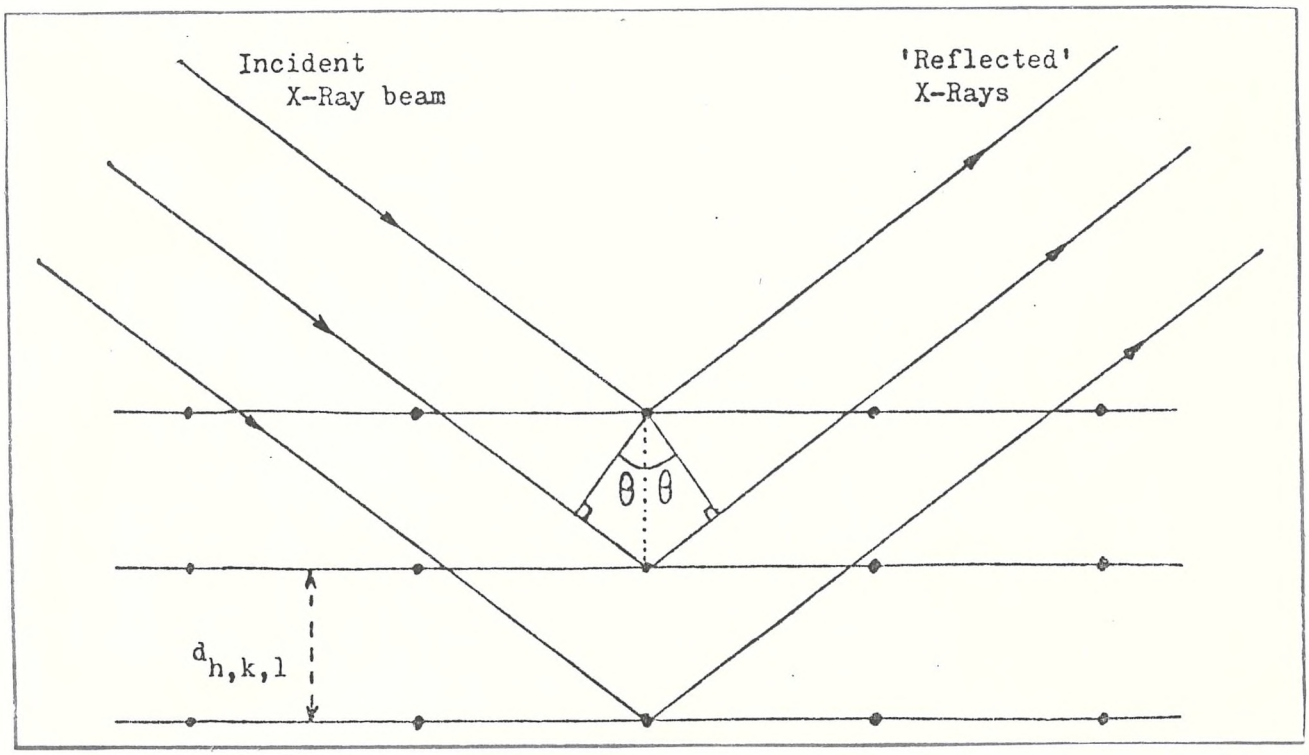

Figure 2.11 The Bragg Conditions.

Figure 2.11 represents successive layers of atoms separated by a distance $d_{(h,k,l)}$. A beam of monochromatic light whose wavelength is less than the separation of atomic planes is incident upon the material at an angle of θ^{o}. Under these conditions it is possible for rays of light diffracted from successive layers to interfere constructively and give rise to a pattern of diffraction spots. From the general condition for constrctive interference and the geometrical arrangement the following relation was derived by Bragg (91).

$$n\lambda = 2\, d_{(h.k.l)} \sin\theta$$

where θ is the angle of incidence of the beam,

$d_{(h.k.l)}$ the distance between successive planes,

λ = the wavelength of the radiation

and n = the order of diffraction.

h, k and l are integer numbers called the Miller indices. They characterise a family of planes by giving the position of one of these planes in the unit cell.

In crystalline materials, the distance between atomic planes is typically of the order of a few Angstroms units (10^{-8}cm) and consequently the appropriate light for observing diffraction should have a wavelength of about one Angstrom. Light of this wavelength falls in the X-ray region of the electromagnetic spectrum.

In the case of powdered or polycrystalline materials a circular diffraction pattern is observed due to the random orientation of the crystal planes within the sample. Crystalline polymers also possess an additional type of layer or periodicity as a result of differences in electron density between crystalline and amorphous zones. The periodicity of this type corresponds to 50-1000 Angstroms units and gives rise to diffraction at very small angles of 2^{o} 2θ - 6' 2θ, respectively.

The main application of X-ray diffraction in this present study was in obtaining a measure of relative crystallinity in polymer samples. This was carried out by comparing the intensity of X-rays diffracted by the crystalline portion with the diffraction from the amorphous portion.

Traces of variation of intensity with diffraction angles are obtained from X-ray photographs by means of a microdensitometer and the areas under the curves are most easily estimated by means of a curve resolver. A background line is chosen between two points at which the polymer shows diffraction minima. This line as well as the crystalline and amorphous peaks are reproduced from the microdensitometer trace by means of the curve resolver. The relative crystallinity is then estimated from the

ratio of the area under the crystalline peak and above the amorphous peak to the total area above the background line (92). Broadening of peaks may arise from the finite width of the X-ray and from crystalline imperfections. These same problems occur in the estimation of the size of the crystallites within a polymer sample by the Scherrer equation.

$$L = \frac{K\lambda}{\beta_c \cos\theta}$$

where L is the crystallite size in Angstroms,

K is the form factor, nominally $1^{o}2\theta$,

λ is the wavelength of the incident X radiation in Angstroms,

β_o is the width at half height of the diffraction peak,

θ is the angle of diffraction of the peak.

In all X-ray diffraction experiments $CuK\alpha$ radiation of 1.54 Angstroms was used. The X-rays were produced by means of a Raymex 60 power supply and an Elliot tube. The target in the X-ray tube is made of copper, and a nickel filter is used to filter out the $CuK\beta$ diffraction. The camera uses point collimation and detection is made by taking a flat photograph. A Joyce & Loebel microdensitometer was used to obtain traces of the intensities of the diffraction rings.

For recording photographs at low temperatures, a specially designed cell shown in figure 2.16 was used together with a camera which can be evacuated.

Polymer samples.

Polyethylene samples consisted of Rigidex 9 which is solution polymerised and available in granule form. Rigidex 006-60 a particle polymerised analogue of Rigidex 9 is available in powdered form and was also used in experiments. Both of these polymers have a number average molecular weight of about 10^4. Polyoxymethylene samples consisted of Dupont ex-reactor fluff and Delrin 500 both of number average molecular

weight between 3×10^4 and 4×10^4.

The crystalline melting points of these grades of polyethylene and polyoxymethylene are 146°C and 175°C respectively. The glass transition temperature of polyethylene is approximately -93°C (180K) and that of polyoxymethylene is approximately -78°C (195K).

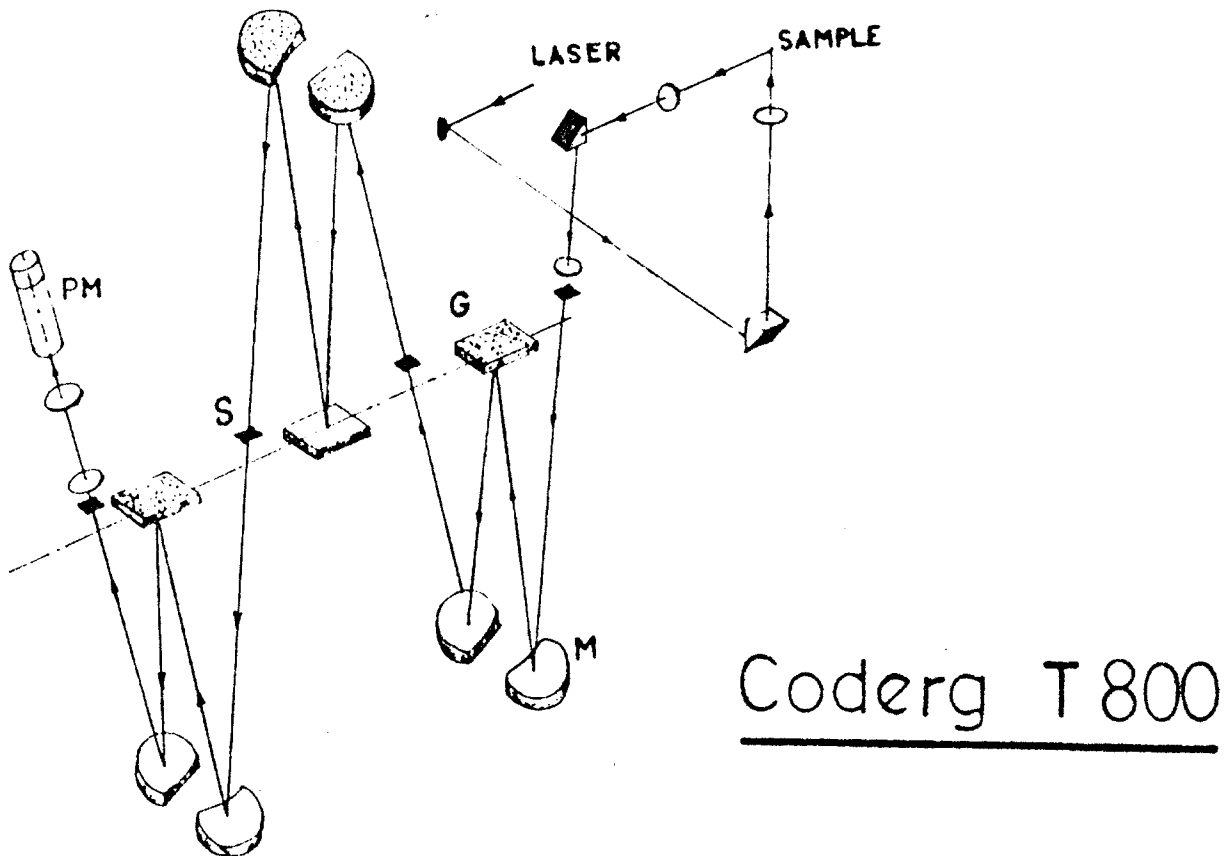

Figure 2.12 Optical diagram of the Coderg T800 Raman spectrometer.

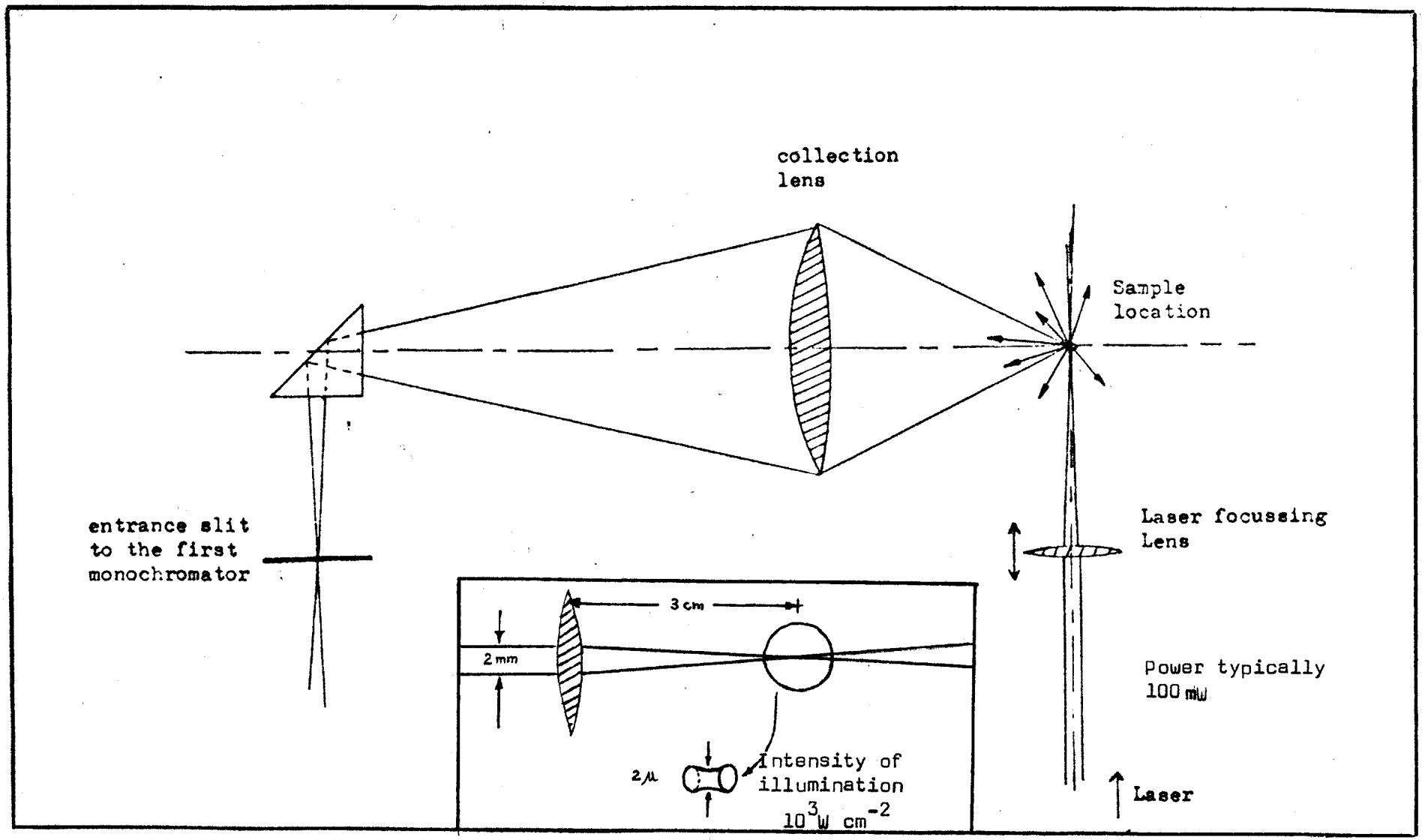

Figure 2.13 Illumination and collection system used in Raman spectroscope experiments.

Inset: Focusing of beam into a sample.

Figure 2.14. Low frequency Raman spectrum of polyethylene showing L.A. mode.

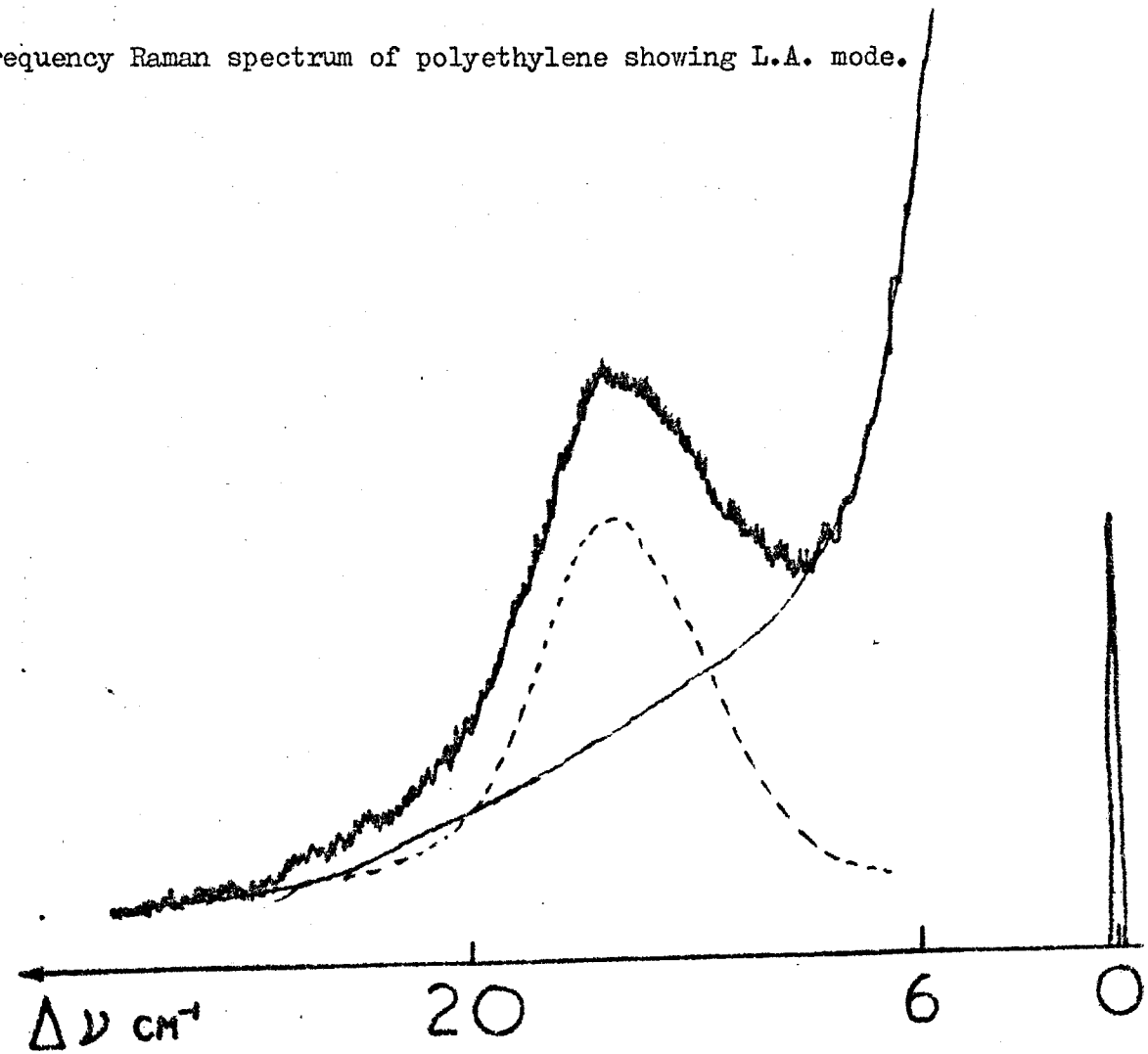

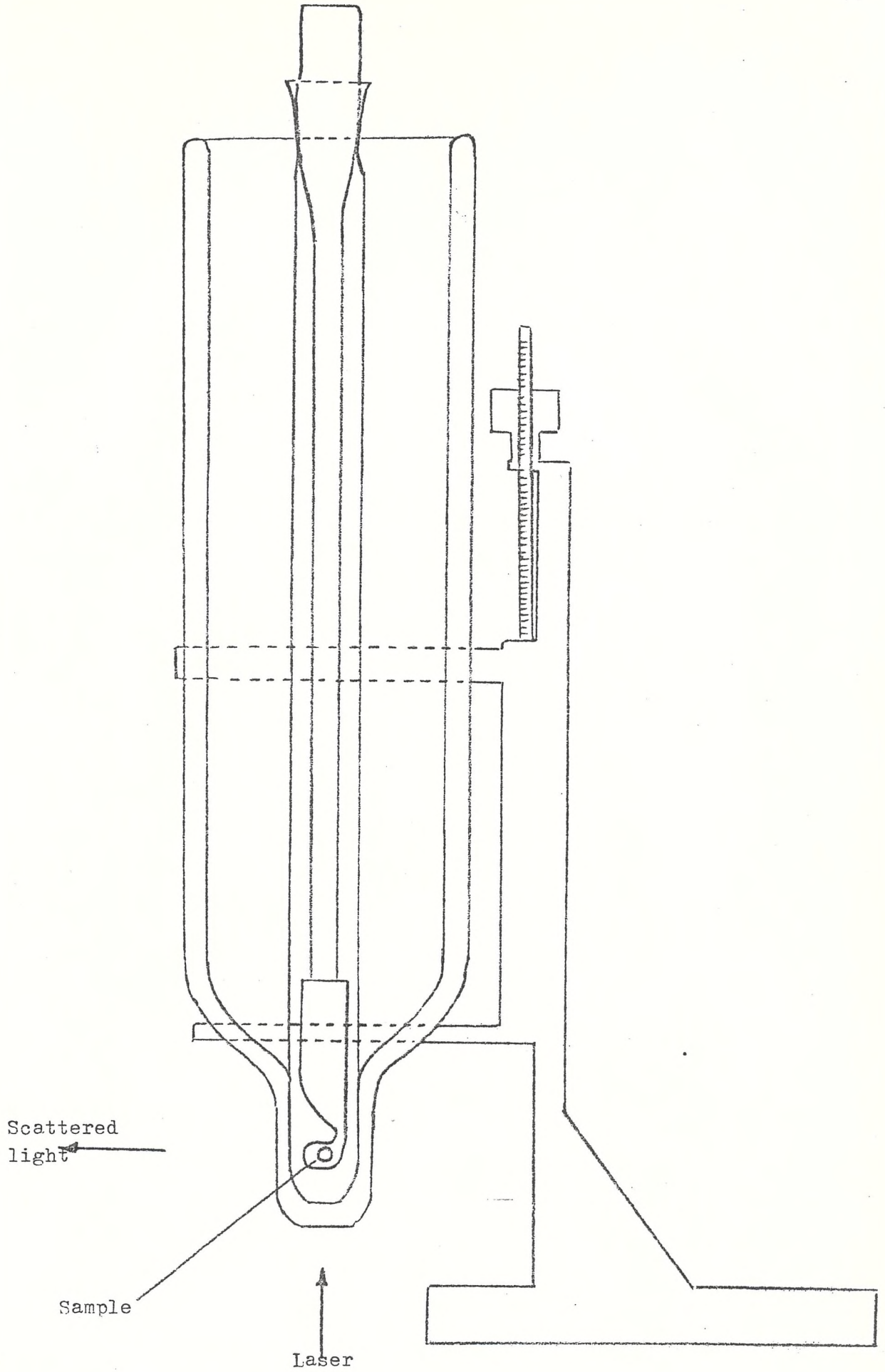

Figure 2.15 Raman spectroscopy cold-cell.

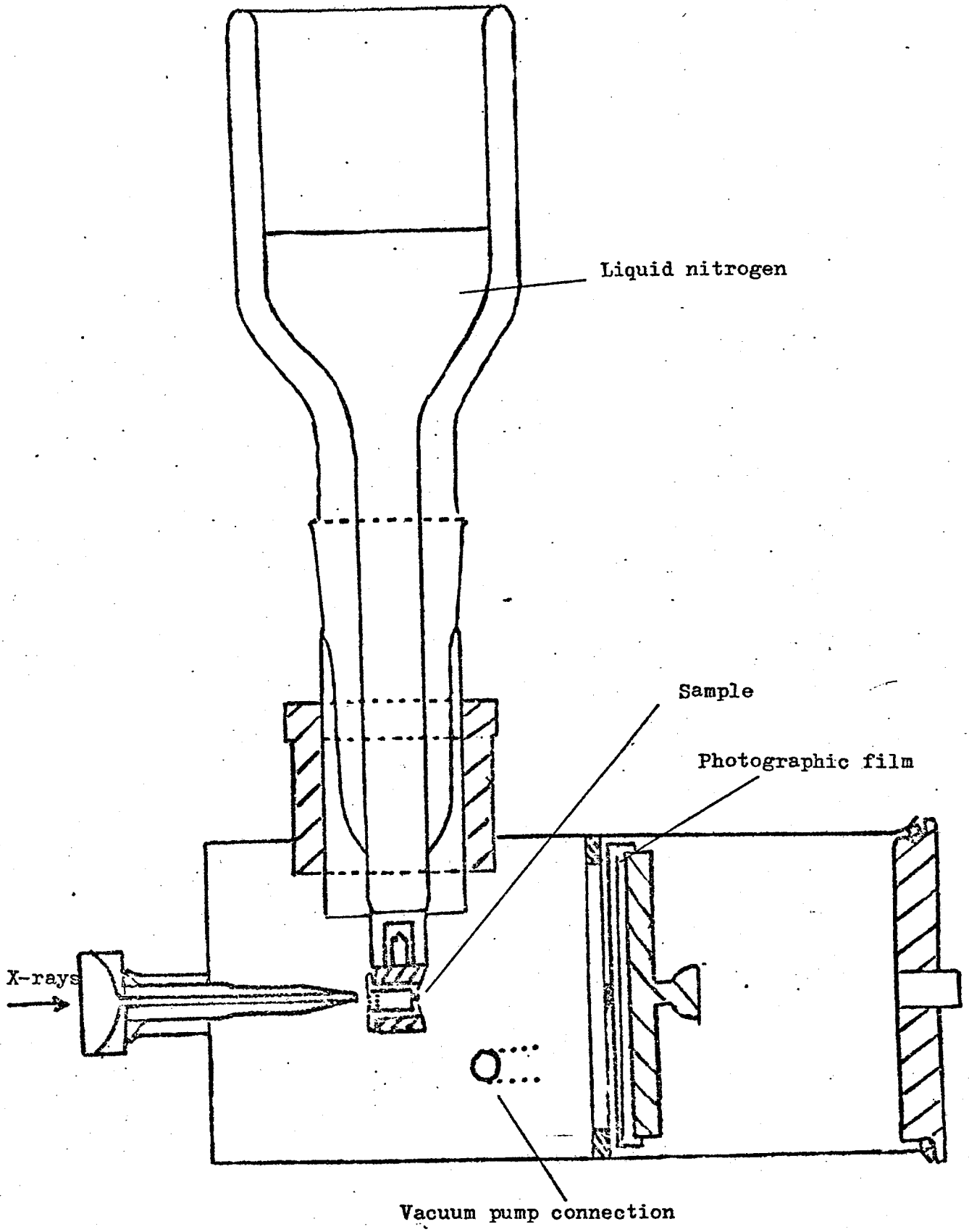

Figure 2.16 Low temperature X-ray cell.

CHAPTER III RAPID COOLING OR "QUENCHING" EXPERIMENTS

It has been observed that in polyethylene which is rapidly cooled from the melt, the lamellar thickness is related to the melt temperature (53). This behaviour is not accounted for by the crystallisation theories based on the folding of polymer chains. These experiments were carried out on high density material which was molten at various temperatures and then quenched at -180°C by immersion in liquid nitrogen. Other modes of quenching were also employed and were found to produce similar changes in the L.A. mode frequencies of the polyethylene samples as those shown in table 3.1.

Table 3.1 L.A. mode frequencies for quenched high density polyethylene melts (53).

Temp. of Melt	Quenched in ice & water LA mode freq. (cm^{-1})	Quenched in CO_2/ alcohol LA mode freq. (cm^{-1})	Quenched in liq. N_2 LA mode freq. (cm^{-1})	Trans. CH_2-CH_2 sector length (Angstroms)
160°C	16.5 ± 0.5	17.0 ± 0.5	17.0 ± 0.5	195 - 179
250	17.5 ± 0.5	18.5 ± 0.5	18.0 ± 0.5	184 - 168
300	18.5 ± 0.5	19.0 ± 0.5	18.0 ± 0.5	175 - 164
350	20.0 ± 0.5	20.0 ± 0.5	19.0 ± 0.5	171 - 156
400	20.5 ± 0.5	21.0 ± 0.5	20.5 ± 0.5	160 - 149

The behaviour of polyethylene with regards to quenching experiments may well be common to other crystalline polymers. Experiments were carried out on polyoxymethylene in order to investigate this notion.

Small samples were heated at the rate of 10 degrees per minute in a differential scanning calorimeter, held for 3 minutes at various temperatures and then rapdily quenched into a refrigerant. Another set of samples were prepared by cooling in the calorimeter which was operating at a cooling rate of 320 degrees per minute.

In each case the polymer samples were removed from the D.S.C. pans after they had been allowed to warm to room temperature and Raman spectroscopy was used to measure the L.A. mode frequencies at room temperature. The results of these experiments on Dupont ex-reactor fluff are shown in Table 3.2

Table 3.2 Observed L.A. mode frequencies for polyoxymethylene quenched from melt into liquid nitrogen (-180°C), ice/water mixture (0°C), and cooled at 320 degrees per minute.

Melt Temperature (°C)	L.A. mode frequency (cm^{-1})		
	Quenched in liquid nitrogen	Quenched in ice/water	Quenched at 320°/minute
182	12.5 ± 0.5	13.0 ± 0.5	11.5 ± 0.5
202	13.0 ± 0.5		
222	14.0 ± 0.5		
242	14.5 ± 0.5		
262	16.0 ± 0.5	16.0 ± 0.5	13.0 ± 0.5

Measurements were also carried out on commercially available Delrin 550 grade of polyoxymethylene. A similar change in the L.A. mode frequency of 3 cm^{-1} was observed over the same melt temperature range as in Table 3.2 after quenching in liquid nitrogen.

Low angle X-ray diffraction measurements were carried out (by Dr. D. Blundell at I.C.I.) on polyoxymethylene samples moulded and rapidly quenched at Southampton. The data was obtained using a Kratky camera fitted with a position sensitive detector. After "slit desmearing" and a Lorentz correction the position of the diffraction peak maximum was used to determine the Bragg long period (93). The L.A. modes of the same samples were observed and are shown together with the corrected long spacing derived from L.A.X.D.

Table 3.3 Lamellar thickness estimated by low angle X-ray diffraction and L.A. modes in quenched samples of polyoxymethylene.

Melt Temperature (in ^{o}C)	Lamellar thickness from L.A.X.D. (Angstroms)	L.A. mode (cm^{-1})
185	158 ± 10	12.0 ± 0.5
225	151 ± 10	13.0 ± 0.5

Critics of the quenching experiments carried out at Southampton have suggested that although the lamellar thickness observed by Raman spectroscopy may indeed increase with melt temperature, that the overall lamellar thickness does not do so. This would require a compensating decrease in the thickness of the amorphous region so that the overall effect would be one of a change in the proportion of the two phases as a function of melt temperature. It was shown that this behavious does not occur by the following experiment.

A measure of the crystallinity obtained by high angle X-ray diffraction is given by the expression:

$$\text{Crystallinity} = \frac{l_c}{2l_f + l_c}$$

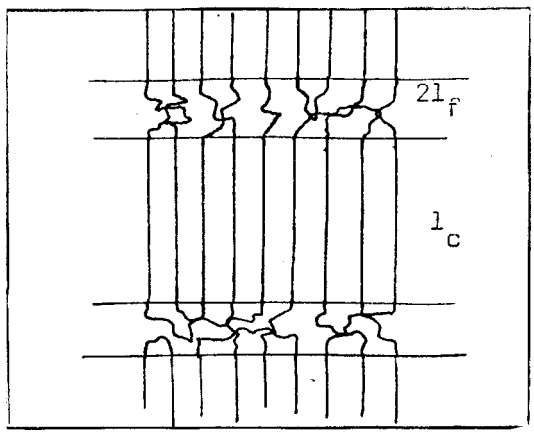

Figure 3.1

where l_f + the half thickness between the lamellar cores of thickness l_c. Hence $2l_f + l_c$ = the long spacing. If the latter remains constant the observed crystallinity should be directly proportional to l_c. The X-ray crystallinities of three of the polyoxymethylene samples quenched in liquid nitrogen were obtained by standard procedures and the results are shown in Table 3.4. Corresponding values of the L.A. modes obtained by Raman spectroscopy are also contained in Table 3.4.

Table 3.4 High angle X-ray crystallinities of polyoxymethylene samples quenched from different melt temperatures into liquid nitrogen.

Melt Temperature (^{o}C)	L.A. mode (cm^{-1})	$l_c/2l_f + l_c$
182	12.5 ± 0.5	0.64 ± 0.1
222	14.0 ± 0.5	0.68 ± 0.1
262	16.0 ± 0.5	0.65 ± 0.1

These results show a lack of direct proportionality between crystallinity and the lamellar thickness (proportional to l_c) and suggest that the "quenching effect" is not caused by a change in the ratio between the crystalline and amorphous content. The theories of crystallisation predict that lamellar thickness is governed by nucleation density. This aspect of the theories was also investigated by examining the relationship between temperature variation of nucleation density and lamellar thickness. The heating of polymer samples leads to a loss of nucleation sites and consequently spherulites observed microscopically are fewer and larger in size. This behaviour was observed in polyoxymethylene and furthermore the number of spherulites remained depleted when a thin film was re-melted and quenched from a lower temperature. The L.A. mode value however appears to be independent of nucleation density because after re-melting and quenching from a lower temperature it reverted to a high value.

Table 3.5 contains the observations made in these experiments.

Table 3.5 The effect of heat treatment on the nucleation density and L.A. mode in film samples of polyoxymethylene.

Melt Temperature of film sample (^{o}C)	L.A. mode (cm^{-1})	Number and size of spherulites
185	14 ± 0.5	Large number, small
250	16 ± 0.5	Small number, large
Re-melted at 185	14 ± 0.5	~~Large~~ Small number, ~~small~~ large

It is not strictly possible to identify the L.A. mode with the crystalline core thickness in polyoxymethylene, but it gives a measure

of lamellar thickness which includes some amorphous material. The contribution of the amorphous phase was however found to be very small as samples of polyoxymethylene showed the same lamellar thickness both at room temperature and at -180^{o}C. The Young's modulus of the amorphous phase of polymers is known to be sensitive to changes in temperature and to produce a change in the L.A. mode frequency if the amorphous phase contributes significantly to the L.A. mode vibration (94). Furthermore considering the Raman and low angle X-ray data together, polyoxymethylene does appear to show a behaviour similar to polyethylene on quenching from the melt. For very rapid quenching, the rate of cooling does not significantly influence the observed change in L.A. mode and hence lamellar thickness as defined above. This behaviour is contrary to the theories of crystallisation based on a chain folded structure in which the degree of supercooling determines the resulting lamellar thickness. The slower rate of 320 degrees per minute produces a smaller change in the L.A. mode frequency as was found to be the case with polyethylene (53). It has been shown that both cooling rate and nucleation density alone do not govern the observed lamellar thickness of the polymer. Both of these factors contribute to the degree of supercooling thus suggesting that the crystallisation theories may be in error when applied to crystallisation from the melt.

It is therefore necessary to consider an alternative model which incorporates a high degree of crystallinity as well as the presence of lamellae, but in which chain folding is not predominant. The solidification model described in Chapter I provides a more appropriate description of the structure of polyoxymethylene as in the case of polyethylene. The interlamellar regions contain polymer chains which connect adjacent lamellae although chain folding and re-entry of the same lamella may occur to a small extent.

Similar experiments were carried out on polyethylene oxide, but no change was found in the L.A. mode frequency as a function of melt temperature. The samples used were those of low molecular weights (1000, 2000, 3000) which have experimentally accessible L.A. modes. The results of these experiments are contained in Table 3.6. High molecular weight P.E.O. was also examined but its L.A. mode is at 6 cm^{-1} and is too close to the Rayleigh peak to allow any accurate measurements to be made.

Table 3.6 L.A. modes of polyethylene oxide observed after quenching from the melt into liquid nitrogen.

Melt Temperature (^{o}C)	L.A. mode frequency (cm^{-1})		
	P.E.O. 1000	P.E.O. 2000	P.E.O. 3000
65	18.0 $\pm$ 0.5	9.0 $\pm$ 0.5	12.0 $\pm$ 0.5
130	18.0 $\pm$ 0.5	9.0 $\pm$ 0.5	12.0 $\pm$ 0.5
200	18.0 $\pm$ 0.5	9.0 $\pm$ 0.5	12.0 $\pm$ 0.5

The lack of a "memory effect" in this study may indicate a dependence upon molecular weight contrary to some earlier findings (95). It was found that polyethylene of very high molecular weight produced the same changes in lamellar thickness as in commercial polyethylene following quenching from the melt. As the article pointed out, the L.A. modes of these samples were very broad, but it was nevertheless concluded that the molecular weight of the polymer was not a factor in determining the lamellar thickness produced.

Some authors believe that polymers of low molecular weight are chain folded and evidence has been published to support this view in the case of polyetnylene oxide (96).

Hartley et. al. concluded that polyethylene oxide of M_n = 2000 or less crystallises in the chain extended form and that of M_n = 4000 or higher in the chain folded form. Fractions of M_n = 3000 was thought to contain both types of crystals.

The production of a glass phase of polyoxymethylene.

The glassy phase possesses an amorphous structure characteristic of a liquid although it is actually in the solid state. This type of phase is produced when a molten material is cooled so rapidly as to prevent rearrangement of molecules into a more ordered crystalline state. Polymeric galsses are readily formed and maintained even at room temperature by some materials such as polystyrene. The large side groups of these molecules prevent the ordering of chains and thus favour the formation of a glass. Polyethylene and polyoxymethylene do not possess large side groups and crystallise quite readily as the temperature of the molten polymer is reduced. Indeed until relatively recently it was considered impossible to produce a glass of polyethylene. As mentioned in Chapter I, certain theories of polymer crystallisation based on the chain folding model predicted that irrespective of the supercooling rate achieved a truly amorphous or glassy phase of polyethylene could not be produced.

In 1975, however, Hendra et. al. succeeded in achieving just that and thus provided some further evidence against the chain folding model (97). These authors used a highly specific heat treatment whereby the temperature of the polymer melt was reduced extremely rapidly by quenching into liquid nitrogen and without allowing it to warm to a temperature above 120K. The phase obtained thus was shown to be a glass by spectroscopic techniques. Infra-red spectra taken at various temperatures as the glass was warmed showed that at 180K the correlation (or Davydov) splitting effect appeared at a prominent band.

This behaviour shows the transition from the glassy structure to that of crystallinity. Later work provided an X-ray diffraction pattern of a similarly quenched polyethylene sample which showed a broad peak characteristic of the amorphous phase (98).

As it has been shown that polyoxymethylene displays similar trends to those of polyethylene with regard to the lamellar thickness obtained on quenched from the melt, it would seem reasonable that a glass of polyoxymethylene can also be obtained. The glass transition of the two polymers are also very similar (polyethylene 180 K and polyxoymethylene 195 K). However, the characterisation of a glass of P.O.M. by infra-red spectroscopy is not so readily achieved because the more stable modification of this polymer possesses only one chain per unit cell. The correlation splitting effect arises from the interaction between neighbouring chains within the same unit cell and is thus absent in polyoxymethylene (99). It was therefore decided to obtain an initial characterisation from X-ray diffraction experiments. Figure 3.3 illustrates the broadening of the X-ray diffraction peak upon the formation of the glass phase. In this case the polymer is polypropylene which shows two peaks in its paracrystalline state and one broad peak in the glassy state (100). Similarly in polyethylene two sharp peaks are observed in the crystalline phase and a single broad peak in the glass (98).

The following experimental procedure was carried out with polyxoymethylene. A thin film sample was pressed at 200^{o}C then dropped into liquid nitrogen. A small sample was cut and transferred into the cooled sample holder of a specially designed low temperature X-ray cell. (Figure 3.2). This procedure was carried out under liquid nitrogen and because of difficulties in manipulation several attempts were made to obtain the glass. The film exposure times of one hour were used. Traces of scattering intensity as a function of angle were obtained from the photographs by means of a microdensitometer. These were compared with the traces obtained from the same sample which had been allowed to

warm to room temperature and which therefore had a crystalline structure. Precautions were taken to prevent the formation of ice crystals around the sample, but this did occur to a small extent and caused a deterioration in the photographs and consequently of the diffractometer traces. The microdensitometer traces showed considerable differences between the crystalline and suspected glass phases. The crystalline phase had a single sharp peak at 23^{o} 2θ characteristic of hexagonal polyoxymethylene. The glass phase produced a broader trace with an intensity maximum at the lower angle of 22^{o} 2θ. This broadening does not in itself prove the existence of a glass phase and could be explained by the formation of smaller crystallites. The observed change in position of the intensity maximum to a smaller diffraction angle is characteristic of amorphous scattering (98). The use of microdensitometer traces is known not ot provide a very accurate means of comparing intensities. The X-ray photographs themselves show more clearly the contrast in sharp diffraction (crystalline) and broad diffraction pattern (glass) as shown in figure 3.2.

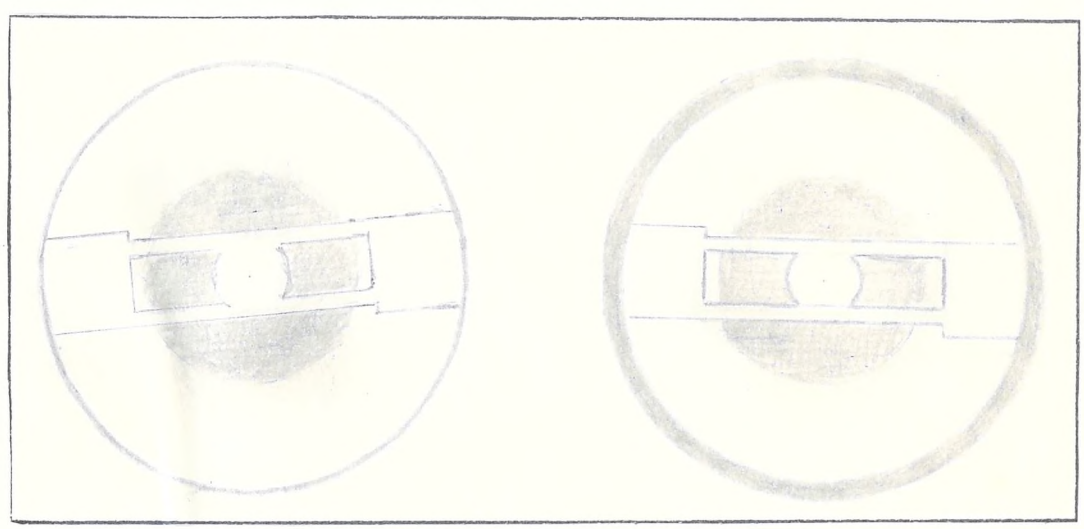

Figure 3.2 Representation of X-ray photograph of polyoxymethylene
crystalline phase (left)
glassy phase (right).

It is also possible to compare the form of the Raman spectra obtained from the molten polymer and those from samples which are quenched and maintained under liquid nitrogen. If these spectra are found to be similar they provide additional evidence for the formation of the glassy phase. Unfortunately it was not possible to complete this experiment as only the Raman spectrum of the molten polymer was successfully obtained (see figure 3.4). Several attempts were made to produce a Raman spectrum of the glass phase. The source of the problem was one of scattering from the two glass interfaces of the cold cell. The spectrum of molten polyethylene was obtained by means of a high temperature cell. Heat was supplied by means of a Controls and Automation temperature controller and a chrome-alumel thermocouple was used to obtain an accurate estimate of the temperature of the sample. The peaks in the crystalline spectrum were assigned to molecular vibrations with tne aid of reference (101). The considerable differences in the crystalline and melt phase spectra arise from the appearance of additional rotational isomers in the latter. This behaviour has been previously noted in another helical polymer polyethylene oxide (102) where the disordered helix of trans, trans, trans conformation appears in the melt. The trans, gauche, trans helix typical of the crystalline state is also less predominant (103).

Table 3.7 Assignment of P.O.M. crystalline phase spectrum.

frequency in cm^{-1}	vibrational mode
920	C-O-C symmetric stretching
1110	CH_2 rock + COC symmetric stretching
1340	CH_2 twist
1500	CH_2 bend

Although a complete characterisation of the glass was by no means achieved in the time available the X-ray evidence clearly shows that it is quite possible to obtain this phase.

The quenching experiments described in this chapter are of some industrial relevance as the large scale manufacture of polyoxymethylene also involves rapid quenching from the melt. It would seem that although a great deal of research has been carried out on idealised laboratory materials (or single crystals), a satisfactory theory of "useful" polymers does not exist.

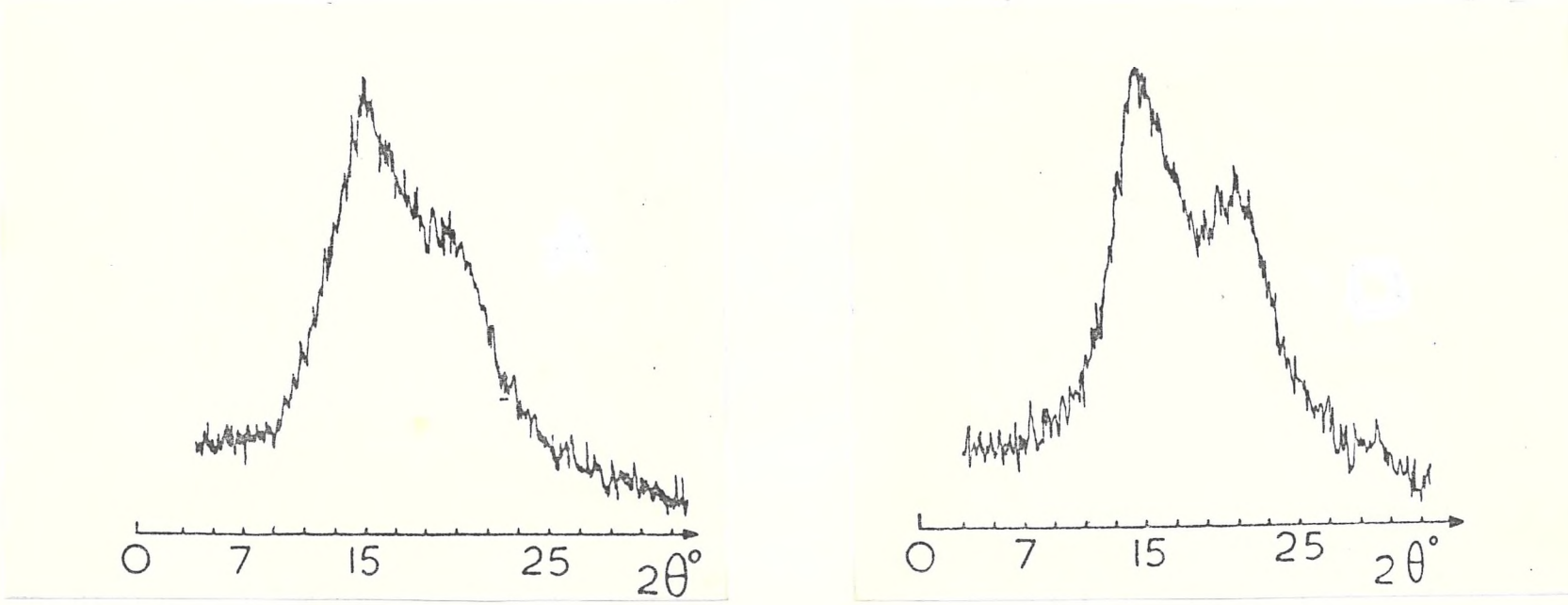

Figure 3.3 Microdensitometer traces from X-ray photographs of isotactic polypropylene:
(left) quenched from 453K into liquid nitrogen, and
(right) quenched from 453 K to 193K and then warmed to room temperature
(paracrystalline phase) (100)

Figure 3.4. P.O.M. Microdensitometer traces from X-ray photographs of film samples slowly cooled (left) and rapidly quenched (centre and right).

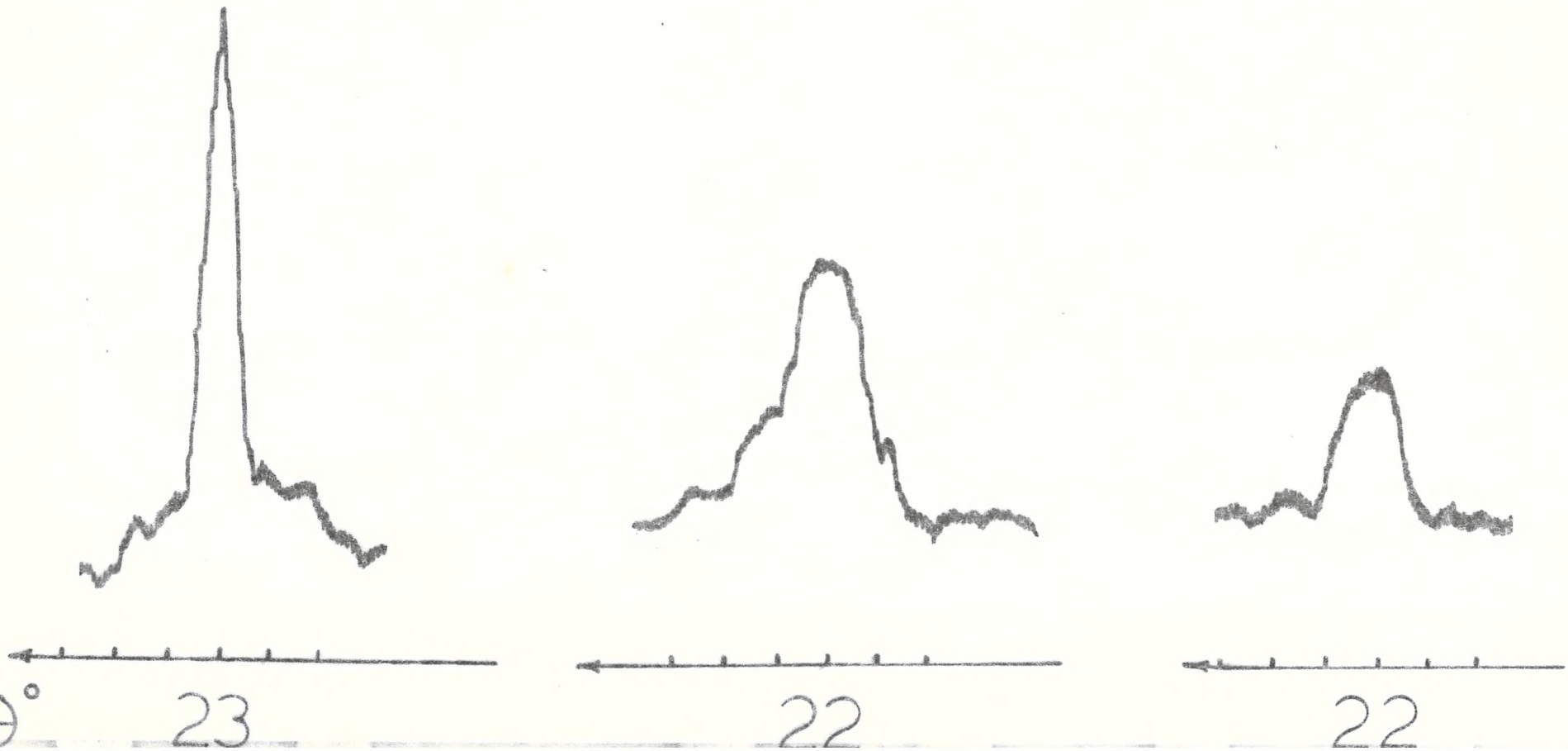

Figure 3.5. Raman spectra of polyoxymethylene recorded at 190°C (A) and 30°C (B).

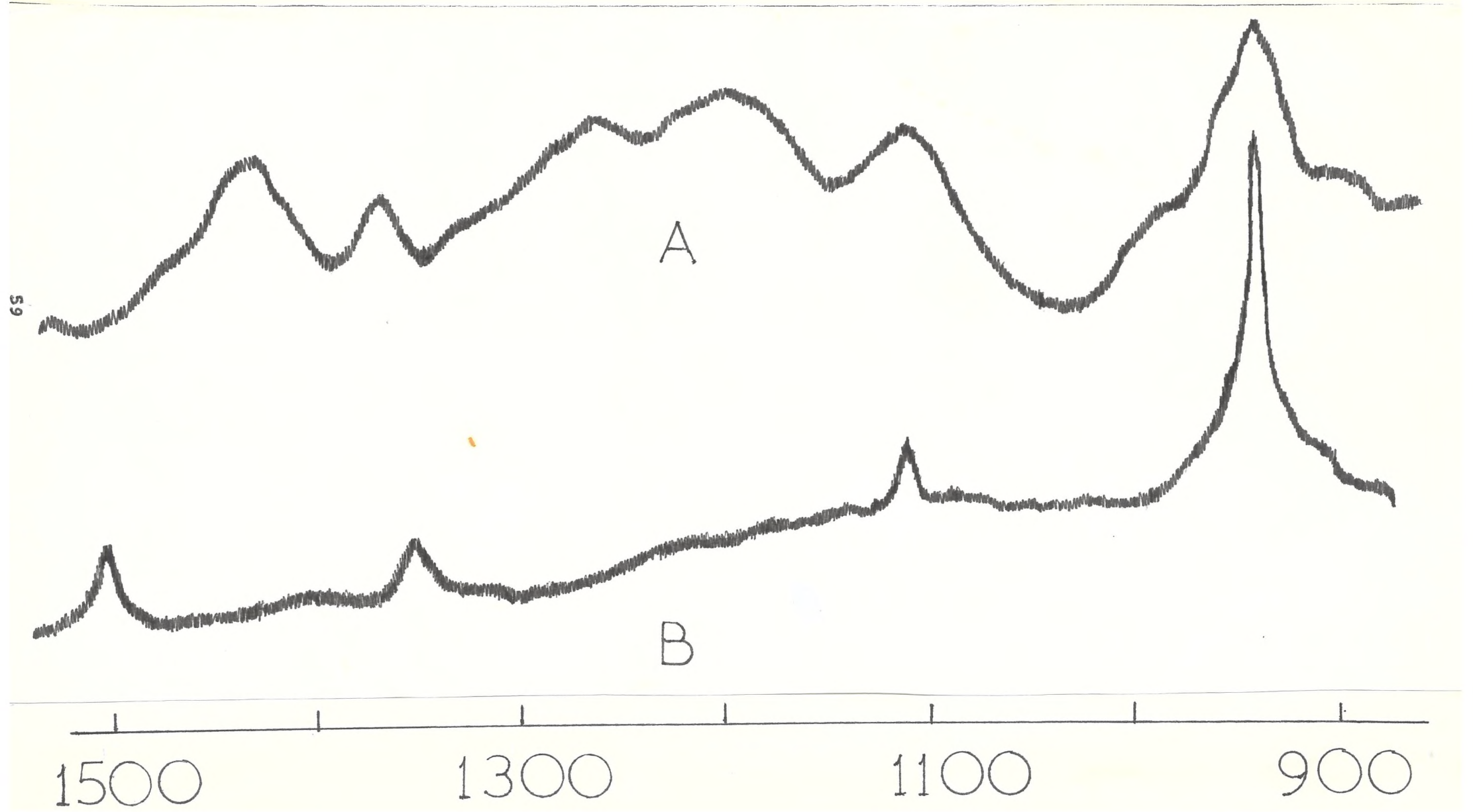

CHAPTER IV THE ROLE OF ENTANGLEMENT IN POLYMER CRYSTALLISATION

Polymer samples were isothermally crystallised from the melt and from solution so that they would possess a different degree of entanglement from material rapidly crystallised from the molten state.

Single crystal matts of polyethylene were prepared by making a 0.05% solution of Rigidex 9 grade in xylene and refluxing until the solid material had dissolved. A hot solution was transferred into a test tube which was suspended in a thermostat bath set at 70°C. After a period of about 2 days the contents of the tube were slowly filtered under vacuum in order to obtain a well oriented matt. The lamellar thickness of these samples was measured by observing Raman active longitudinal accoustic vibrations. Polyethylene was crystallised isothermally by means of a differential scanning calorimeter or by suspending samples in a heating bath at a pre-set temperature. The latter method was favoured in cases where periods of more than one day were required for complete crystallisation. At temperatures below 120°C, crystallisation was carried out by heating small samples of the polymer in D.S.C. pans to 146°C followed by cooling at a very slow rate of 0.31°/ minute to the crystallisation temperature. Samples were subsequently left for twenty-four hours and finally taken out of the calorimeter and allowed to cool to room temperature. The L.A. mode of a sample of Rigidex 9 crystallised at 117°C was found to have a value of 8.5 ± 0.5 cm^{-1}. Solution crystallised and melt isothermally crystallised samples thus prepared were then melted and quenched from a range of melt temperatures into suitable refrigerants. Low frequency Raman spectra were recorded in order to determine the position of the L.A. mode. The findings are shown in Table 4.1.

Table 4.1 Longitudinal accoustic frequencies of quenched melts of polyethylene, Raman data *.

Melt Temperature (in ^{o}C)	Stock polymer melted and then		Crystallised isothermally at 117^{o}C, melted and then quenched to -180^{o}C	Solution crystallised at 70^{o}C, melted and then	
	quenched to 0^{o}C	quenched to -180^{o}C		quenched to 0^{o}C	quenched to -180^{o}C
150	16.5 $\pm$0.5	17.0 $\pm$0.5	15.5 $\pm$ 0.5	18.5 $\pm$0.5	18.0 $\pm$0.5
250	18.5 $\pm$0.5	18.0 $\pm$0.5	16.5 $\pm$ 0.5	19.5 $\pm$0.5	19.0 $\pm$0.5
350	20.5 $\pm$0.5	20.5 $\pm$0.5	17.0 $\pm$ 0.5	20.5 $\pm$0.5	20.0 $\pm$0.5

* All samples were held for 3 minutes in the melt before quenching, Before melting and quenching the stock polymer, isothermally crystallised and solution crystallised polymer had L.A. modes of 15.0 $\pm$ 0.5 cm^{-1}, 8.5 $\pm$ 0.5 cm^{-1} and 28.0 $\pm$ 0.5 cm^{-1} respectively.

It was necessary to ensure that the difference in the variation of the L.A. modes was not simply a consequence of the different initial lamellar thicknesses in the three sets of experiments. Solution and isothermally crystallised samples were held in the molten state for different periods of time and rapidly quenched. The L.A. modes were then recorded in order to determine how long the ordered structure was maintained in the melt. The results of these experiments are displayed graphically in figure 4.2.

A second method, that of radiation crosslinking was used to restrict the relative motion of polymer chains. Evacuated sealed tubes containing polyethylene were prepared for this set of experiments in the following manner. Two sets of four glass tubes provided by the glassblowers were

filled with granules of Rigidex 9 high density polyethylene and simultaneously evacuated to a pressure of approximately 10^{-4} Torr. Traces of water present were reduced to a minimum by heating with bunsen flame and each tube was subsequently drawn and sealed once a pressure of 10^{-4} Torr was re-established. A vacuum line consisting of both a rotary and diffusion pump was used in this procedure. Sealed glass tubes were taken to the Royal Military College of Science at Shrivenham for irradiation with a Co^{60} source of γ radiation.

The first set of tubes received doses of 1.5 MRd, 6.3 MRd, 30 MRd, and 100 MRd at ambient temperature while the second set of tubes were subjected to 3 MRd, 10 MRd, and 15 MRd at $150^{o}C$.

The sample tubes were returned to Southampton University and broken so that small samples suitable for D.S.C. pans could be obtained.

The heat treatment of samples was carried out in a Perkins-Elmer D.S.C.2 differential scanning calorimeter. Samples were sealed in small aluminium pans and nitrogen gas was circulated through the sample holder assembly of the instrument. It was thus possible to heat polymers to well above their melting point without the risk of their decomposing.

After the specimens had been re-melted and quenched from various temperatures the L.A. modes were recorded and plotted (see figures 4.3 and 4.4) together with the L.A. mode at each dosage prior to melting.

The changes in crystallinity which occured in samples irradiated at $30^{o}C$, cooled and then melted and quenched from $150^{o}C$ were estimated by wide angle X-ray diffraction (as shown in figure 4.5). The widths at half height of the peaks were also measured and are shown in Table 4.2.

Table 4.2 Half height widths from X-ray diffraction peaks as a function of radiation dose in polyethylene.

Dose in MRd	Width at half height of (110) peak in degrees 2θ
0	0.6 ± 0.05
1.5	0.6 ± 0.05
6.3	0.6 ± 0.05
30	0.8 ± 0.05
100	0.8 ± 0.05

Irradiation of polymers is also known to cause chemical changes such as oxidation and unsaturation. In order to investigate these reactions, infra-red spectra were recorded on each of the samples irradiated at both 30°C and 150°C. The region between 1,650 cm^{-1} and 1,750 cm^{-1} was scanned and showed no bands characteristic of carbonyl stretching. This feature is not surprising as great care was taken to evacuate oxygen from the samples before they were irradiated. The changes in unsaturation were observed from the 800-900 cm^{-1} region of the infra-red spectra. The observed bands were assigned to chain and terminal unsaturation by making use of the table contained in reference (104).

Table 4.3 Hydrocarbon absorption frequencies. Unsaturated groupings.

Structure	Out of plane bending, mode frequency in cm^{-1}
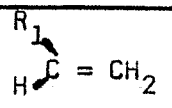	909
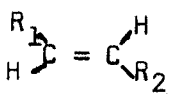	965

The spectra obtained show an increase in chain unsaturation and a decrease in end unsaturation. A quantitative estimate of these changes in unsaturation was made from the infra-red spectra obtained. The number of double bonds per 1000 carbon atoms was obtained from the knowledge of the appropriate band intensities and sample thicknesses (105).

Table 4.4 Number of double bonds (end unsaturation, chain unsaturation) per 1000 carbon atoms in irradiated polyethylene.

Type of double bond	Number of double bonds per 1000 carbon atoms in P.E. irradiated at 30°C			
	0 MRd	1.5 MRd	6.3 MRd	30 MRd
end unsaturation	2	.73	1.25	.2
chain unsaturation	0	.25	.72	.79

Type of double bond	Number of double bonds per 1000 carbon atoms in P.E. irradiated at 150°C		
	3 MRd	10 MRd	15 MRd
end unsaturation	1.80	1.25	.88
chain unsaturation	.12	.23	.68

A measure of the solubility (or gel content) of some of the samples of irradiated polyethylene was kindly provided by the Analytical Laboratories of I.C.I. The samples were exposed to refluxing xylene close to its boiling point while purging with nitrogen gas in order to minimise degradation. The extraction was continued until each sample had attained a constant weight as assessed after drying in an oven at 70°C. The gel content of the samples irradiated at 30°C and 150°C are expressed as percentages in Table 4.5.

Table 4.5 Gel content of irradiated samples of polyethylene

	Polymer irradiated at 30°C		Polymer irradiated at 150°C	
	6.3 MRd	30 MRd	10 MRd	15 MRd
Gel content (percentage)	1.2	73	42	77

It had originally been planned to substantiate these studies on entanglement with some wide-line N.M.R. measurements. After several discussions however it became clear that the latter technique could not be used to study entanglement as a function of melt temperature (106). The use of wide-line N.M.R. in obtaining information on chain entanglement appears to be highly sensitive to the molecular weight distribution of polymers (107). The instruments used in these experiments are furthermore not capable of operating at high temperatures of between 150°C and 350°C.

Figure 4.1 A typical L.A. mode of irradiated polyethylene 15 MRd radiation dose, heated to 250°C, held for 10 minutes and rapidly quenched in liquid nitrogen.

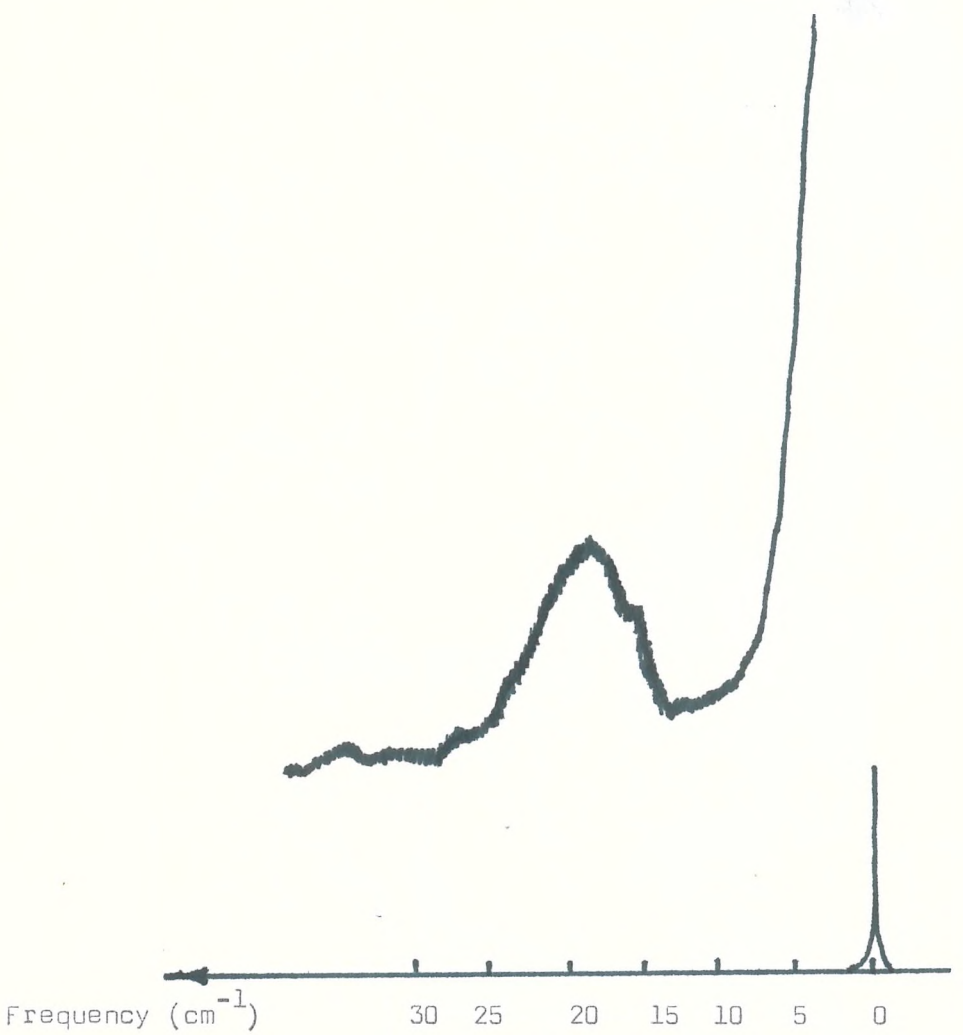

Figure 4.2 Kinetic study of L.A. mode of polyethylene

A solution crystallised
B stock polymer
C isothermally crystallised

each re-melted and held at 250°C for various times before quenching in liquid nitrogen

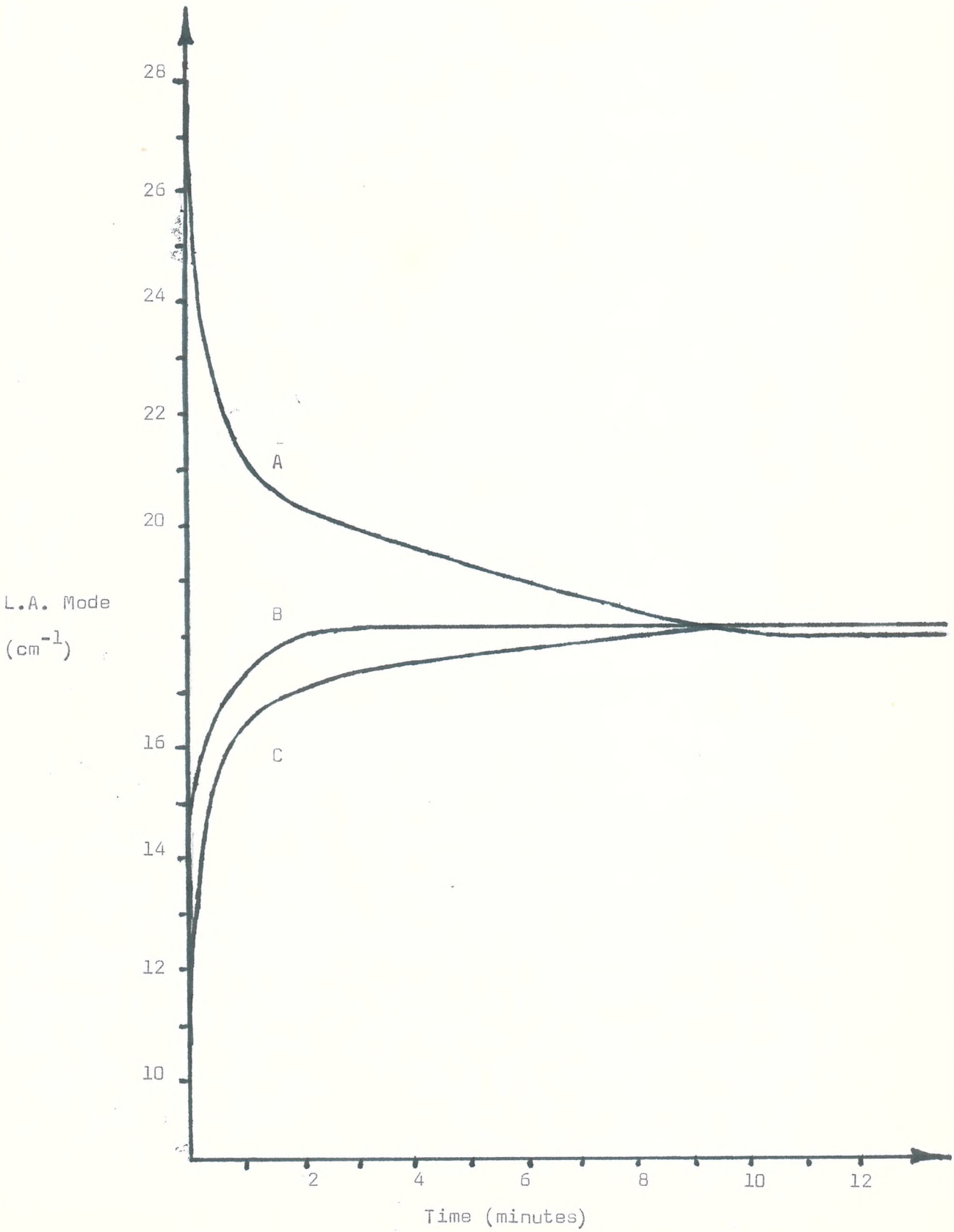

Figure 4.3 L.A. Modes of polyethylene as a function of irradiation dose given at 30°C. Samples re-melted and quenched into liquid nitrogen.

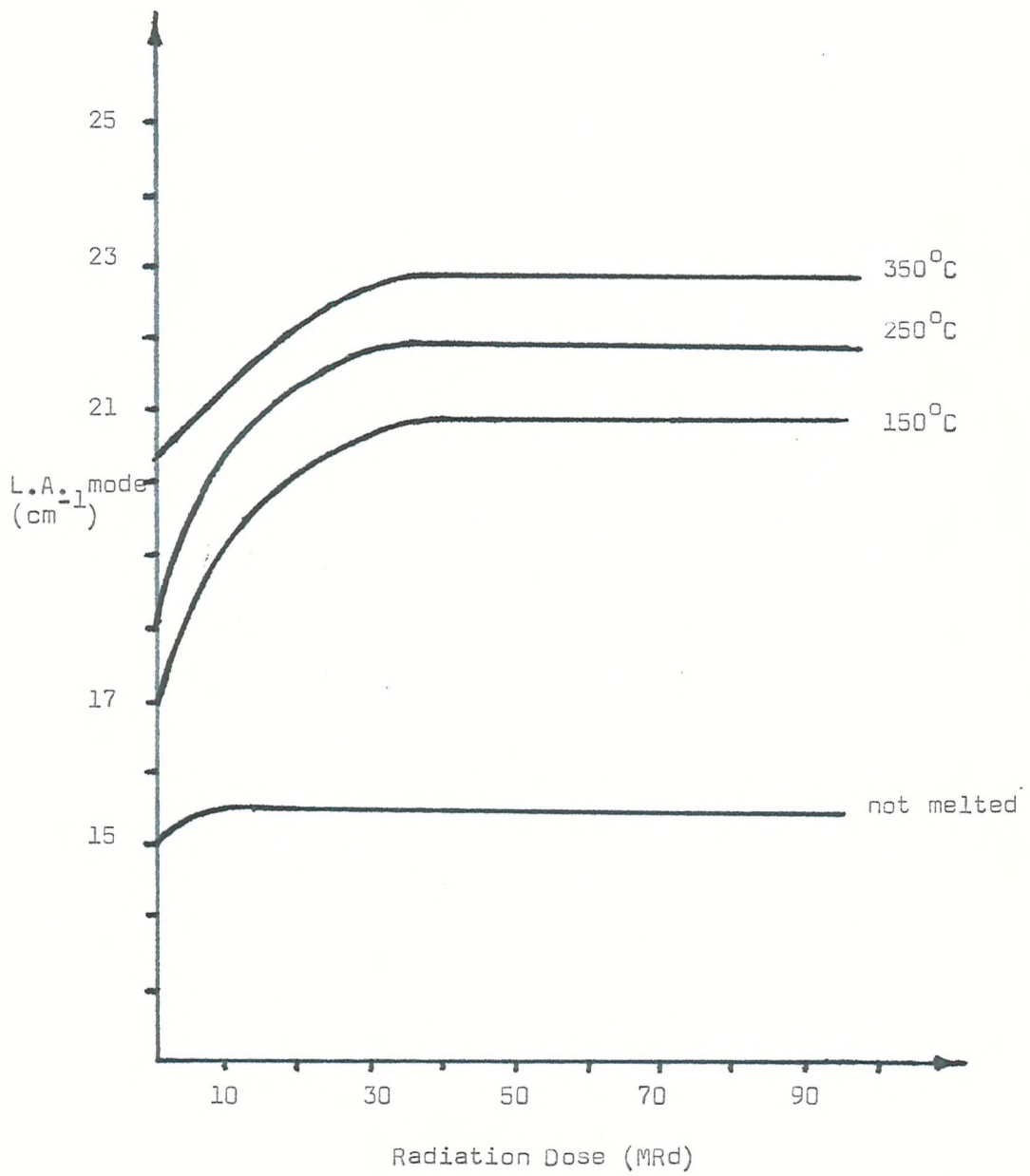

Figure 4.4 L.A. Mode of polyethylene as a function of irradiation dose given at 180°C. Samples re-melted and quenched into liquid nitrogen.

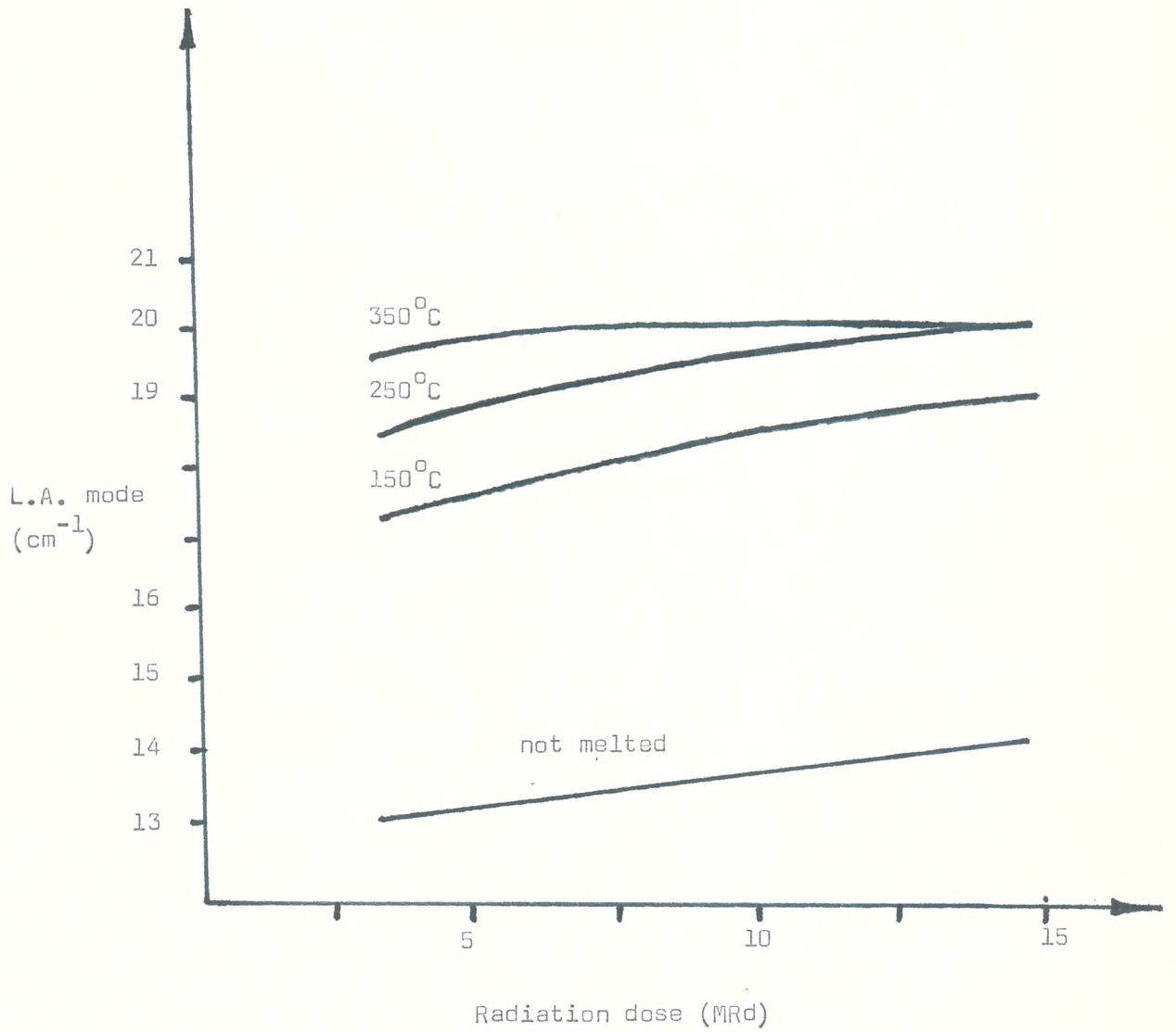

Figure 4.5 X-ray crystallinity of irradiated polyethylene.

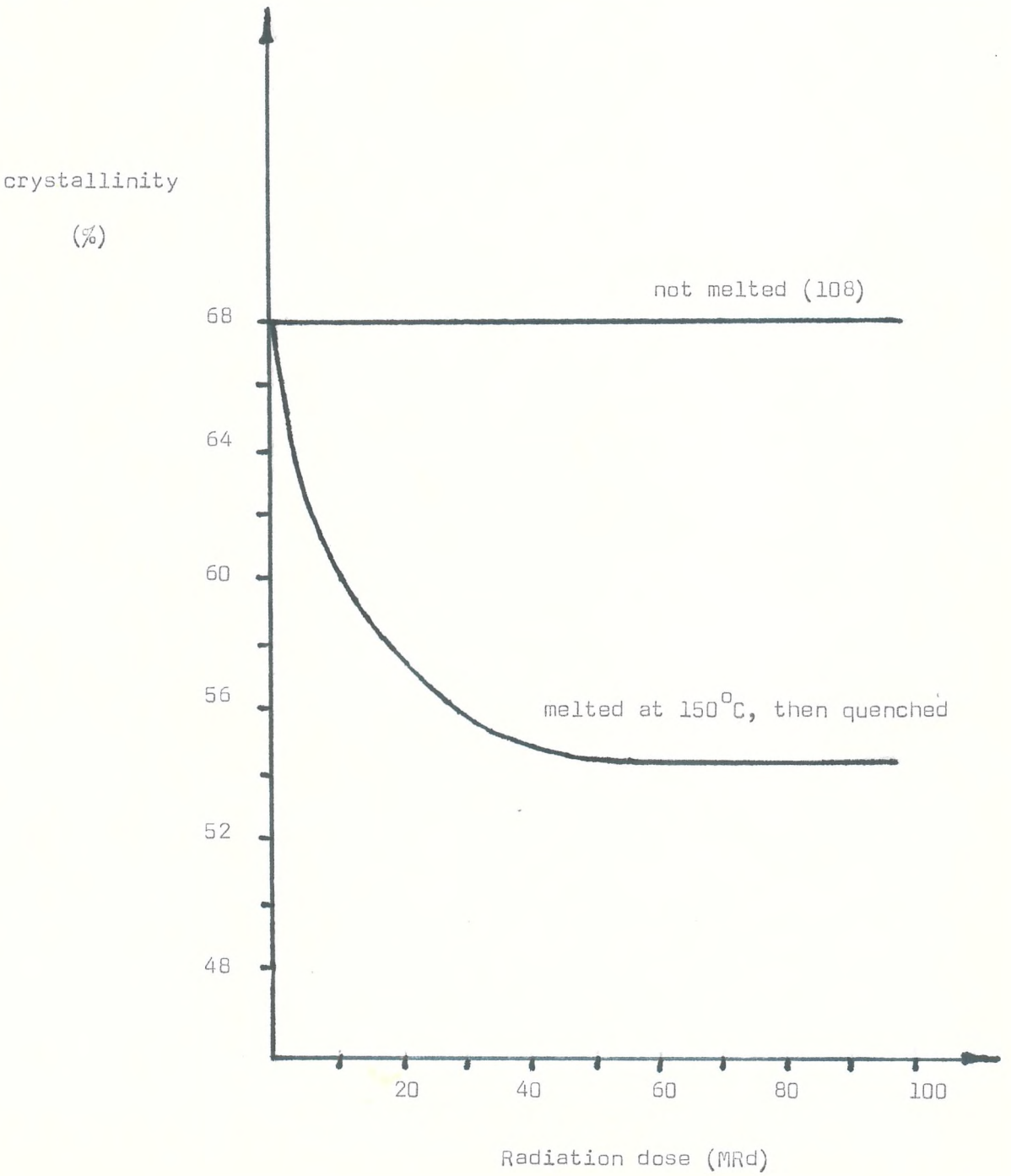

Figure 4.6. Infra-red spectrum of polyothylene film (10 MRd dose at 150°C)

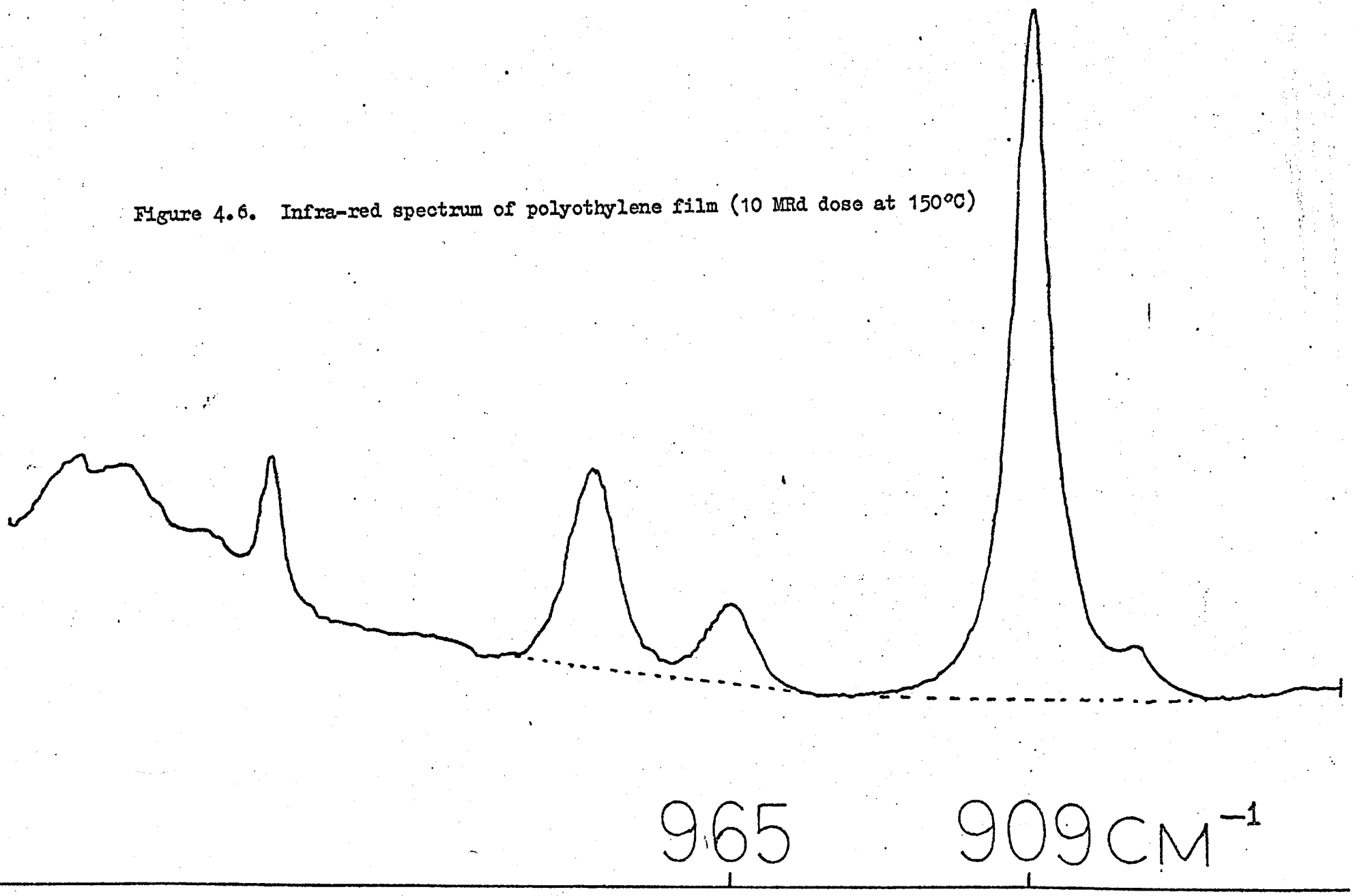

CONCLUSIONS:

1. The mode of crystallisation affects the extent of chain entanglement and consequently the lamellar thickness observed upon rapid crystallisation from the melt (see Table 4.1).

2. The kinetic study (results shown in figure 4.2) showed that the differences in the crystallisation behaviour in the stock polymer, isothermally crystallised and solution crystallised material were not due to differences in initial lamellar thicknesses of the samples used. In the case of the stock polymer no further changes occured in the lamellar thickness after a period of one minute. The isothermally and solution crystallised samples the lamellar thickness changes persisted for a period of approximately ten minutes. After this time the samples acquired the same lamellar thickness as that of the stock polymer. It can therefore be assumed that if the former samples were quenched after a shorter period of time than ten minutes then they would still possess some of the structure due to the original crystallisation process. The data which is contained in figure 4.1 was obtained on samples which had been held in the melt for three minutes prior to quenching and is therefore characteristic of the chain entanglement introduced by the solution and isothermal crystallisation procedures.

3. Similarly, the irradiation of polymers affects their re-crystallisation behaviour and this could also be due to changes introduced into the chain entanglement.

4. The irradiation of polyethylene has a small effect if any on the L.A. mode prior to re-melting , as can be seen in figures 4.3, and 4.4. The X-ray crystallinity of irradiated polyethylene has previously been shown to be unaffected prior to re-melting (108). The Raman spectroscopic results also provide support for the view that when polymers are irradiated the crosslinking occurs predominantly in the amorphous regions (109).

5. The presence of crosslinks does however interfere with the process of re-crystallisation by rapid quenching from the melt as seen by changes in the L.A. mode frequencies (figures 4.3, 4.4.) and the X-ray diffraction studies (figure 4.5). Some studies conducted by De Zarauz several years ago also showed a considerable decrease in the crystallinity of polymers after they had been irradiated and then melted and rapidly quenched from the melt (110).

6. The efficiency of radiation crosslinking appears to be enhanced at the higher temperature of 150^{o}C. This can be seen from both the Raman spectroscopic behaviour (figures 4.3 and 4.4) and the solubility data contained in Table 4.5. A smaller dose of 15 MRd at 150^{o}C is required to produce similar changes in the L.A. mode and gel content to a dose of 30 MRd delivered at 30^{o}C.

7. The findings described in this chapter support a recent theoretical analysis by Rault of crystallisation from the melt phase (111). This author used a Gaussian statistical approach to calculate an average loop length at the θ point of polymer solutions. The loop length is thought to be inversely proportional to the number of entanglements and approximately equal to twice the lamellar thickness (see figure 4.7)

The present study has shown an increase in lamellar thickness with both increasing melt temperature and radiation dose. According to Rault's model these changes could be due to the formation of smaller and more numerous loops in each case.

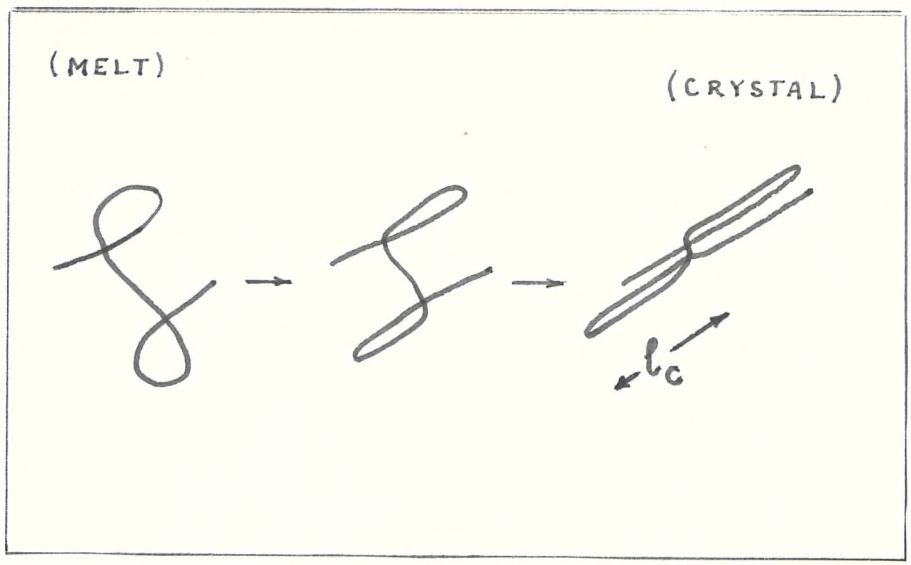

$$l_c = \frac{\text{looplength}}{2}$$

Figure 4.7 Rault's model.
The distance between loops or entanglement determines the lamellar thickness.

8. Finally, the overall trends observed in these studies provide further support for the solidification model polymer crystallisation, and evidence against the regular chain folded model. Entanglements which have been shown to affect the crystallisation behaviour of polyethylene are a feature only of the solidification model. The chain folded model does not provide any explanation of these changes observed upon rapid cooling from the melt. It had been previously suggested that the apparent lack of entanglements in polyethylene observed by E.S.R. spectrsocopy resulted from an absence of tie molecules between neighbouring lamellae (112). These experiments were carried out by drawing polyethylene within the cavity of an E.S.R. spectrometer and monitoring the concentration of free radicals produced. The relative lack of these species was

taken to indicate that regular chain folding predominated in the polymer and that neighbouring lamellae were largely not interconnected. The present Raman spectrsocopic study on entanglement would however suggest that the interconnection of lamellae is present and affects the re-crystallisation of the polymer from the melt.

CHAPTER V RAPID COOLING OF POLYETHYLENE FROM TEMPERATURES BELOW THE MELTING POINT, and speculations as to the factor governing lamellar thickness.

Previous studies of the quenching of polyetnylene have been restricted to rapid cooling from the melt state. As outlined below, tne behaviour of rubber has suggested an extension of the range of observations to include rapid cooling from the solid state.

The behaviour of polyethylene lamellae in contracting when heated has drawn attention to the similarity witn the behaviour of rubber. Most substances show a tendency to expand when they are heated. Rubber is however an exception to this general rule. If a strip of rubber is stretched by means of a suspended weight and heated, it will contract by an amount proportional to the temperature. This effect was first noted in 1805 by Gough, and its understanding contributed to tne development of the theory of rubber elasticity (113).

Figure 5.1 shows tne type of apparatus which may be used to show this behaviour in rubber. A spring with one end free and the other attached to a frame is hooked onto the pointer P pivoted on a support rod R. A rubber band is stretched between a fixed hook X and Y on the spring-pointer arrangement. The band is encased in a glass tube and a contraction is produced when it is heated with a bunsen flame. The change in length of the rubber band is indicated by the movement of the pointer.

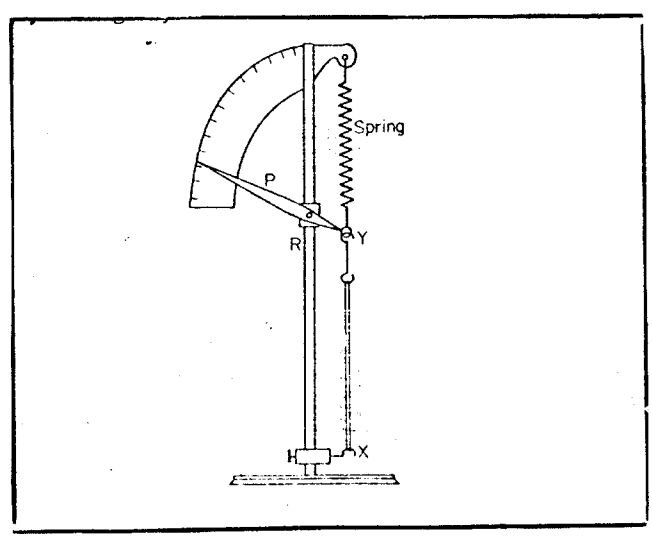

Figure 5.1 Apparatus used to demonstrate Gough-Joule effect (114)

A simplified model of rubber molecules consists of chains of carbon atoms which can adopt different conformations depending on the relative number of trans and gauche units. Studies on simple molecules show that the gauche conformation requires more energy and consequently that raising the temperature of the system produces a decrease in the trans to gauche ratio (114). This same explanation can be used to show how the raising of temperature causes the polymer chains in polyethylene to be more coiled and so possess a smaller all trans segment length, (or an increase in the L.A. mode frequency).

The microscopic analogy in polyethylene would consist of one or more all trans sequences of carbon atoms which are "stretched" between the two ends of the crystalline phase.

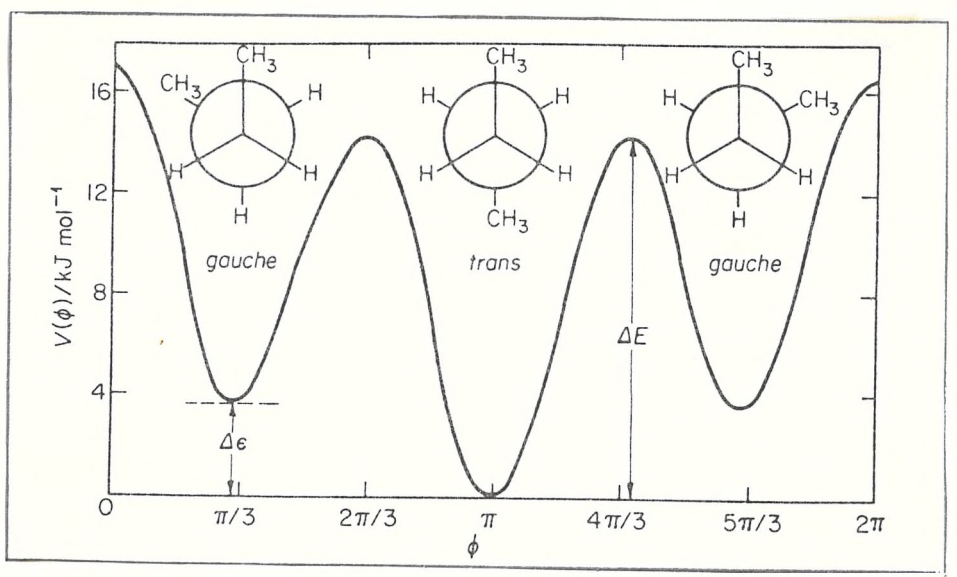

Figure 5.2 Potential energy $V(\phi)$ as a function of the dihedral angle ϕ for-n-butane (114)

In order to determine whether this analogy between rubber and polyethylene has any physical significance the observations on polyethylene were extended to temperatures below the melting point. Experiments were carried out as in the molten state studies by rapidly quenching

polymer samples which had been held for 3 minutes at various temperatures. The L.A. modes were observed by Raman spectroscopy and are shown in Table 5.1.

Table 5.1 Quenching of polyethylene from below the melting point. Observed L.A. modes.

Temperature ^{o}C	Raman Data. L.A. mode in cm^{-1}		
	Quenched in liquid N_2	Quenched into alcohol at -80C	Quenched into ice/water $0^{o}C$
30	15.0 ± 0.5	14.5 ± 0.5	15.0 ± 0.5
85	16.0 ± 0.5	15.5 ± 0.5	16.0 ± 0.5
140	17.0 ± 0.5	17.0 ± 0.5	16.0 ± 0.5
195	18.0 ± 0.5	18.0 ± 0.5	17.0 ± 0.5

These results show that under rapid cooling conditions the "memory effect" does also exist in the crystalline state. It has been suggested that the observed change in the L.A. mode frequency occurs as a result of imperfections in the crystal and not from purely thermodynamic factors (115). The extent to which an annealing mechanism contributes to the observations was investigated by restricting temperatures to well below the melting point. Imperfections were artificially introduced into polymer samples by means of a severe thermal treatment and compared with the behaviour of highly crystalline samples. Three batches of polymer samples were prepared thus and their quenching benaviour was examined:-

(a) Slow crystallisation of polyethylene was carried out in D.S.C. pans by cooling from the melt at the rate of five degrees per minute.

(b) Polyethylene samples were annealed for ten minutes at $125^{o}C$ in the D.S.C. instrument.

(c) Polyethylene samples were held at $250^{o}C$ for five minutes before being rapidly quenched into liquid nitrogen.

Three samples were then taken from each of (a), (b) and (c), warmed to 30°C, 70°C and 110°C in D.S.C. pans, held for 3 minutes and then rapidly transferred into liquid nitrogen. Samples were removed from the refrigerant and allowed to warm to room temperature and the L.A. modes recorded. The more accurate technique of recording the spectra was employed (see Chapter II) in order to reduce the error in estimating the position of the L.A. mode.

Table 5.2 L.A. modes of polyethylene containing various degrees of imperfection, quenched from the solid state.

Held for 3 mins at temperature in °C	Raman data in cm^{-1}		
	slowly crystallised P.E. (Rigidex 9)	Annealed at 125°C P.E. (Rigidex 9)	Imperfections introduced by quenching from 250°C P.E. (Rigidex 9)
30	10.4 ± 0.25	11.2 ± 0.25	17.3 ± 0.25
70	10.7 ± 0.25	11.6 ± 0.25	16.8 ± 0.25
110	11.0 ± 0.25	11.7 ± 0.25	15.0 ± 0.25

Further experiments were carried out on the stock polymer where the effect appears to be more pronounced. For each of the temperatures a control sample was simultaneously heated in the reference sample holder of the calorimeter. Both samples were held for three minutes after which one was rapidly transferred into liquid nitrogen while the other was left in the calorimeter and cooled at a slow rate of 2.5°/minute. The L.A. modes observed in each of six samples are shown in table 5.3.

Table 5.3 L.A. modes of stock polymer (Rigidex 9) heated to temperatures below the melting point before being (a) quenched into liquid nitrogen, (b) slowly cooled.

Temperature ^{o}C	Raman data in cm^{-1}	
	Rapidly quenched into liquid N_2	Slowly cooled at 2.5^{o}/minute
30	15.0 ± 0.25	15.0 ± 0.25
70	16.5 ± 0.25	16.5 ± 0.25
110	17.0 ± 0.25	14.0 ± 0.25

A further experiment was performed in order to ensure that the changes observed in the L.A. mode were not due to the early stages of the annealing process. Samples were maintained at $70^{o}C$ for various periods of time and then rapidly quenched into liquid nitrogen. The results of measurements of the L.A. modes are displayed in Table 5.4.

Table 5.4 L.A. modes of stock polymer (Rigidex 9) heated to $70^{o}C$ and maintained for various times before quenching into liquid nitrogen.

Time in minutes	Raman data in cm^{-1}
3	16.0 ± 0.25
6	16.0 ± 0.25
12	16.0 ± 0.25

It would appear from the data contained in Table 5.2 that the memory effect persists in samples which have a relatively high crystal perfection while

polyethylene possessing crystal strain shows a behaviour typical of annealing experiments, i.e. thickening of lamellae and a reduction in the L.A. mode frequency. Furthermore, a comparison with Table 5.1 shows that the effect is less pronounced. This fact is not unreasonable in view of the experiments described in Chapter IV where it was found that more ordered polymers showed approximately half the change in L.A. mode frequency than that observed in the stock polymer.

The findings shown in Table 5.3 suggest that the thermal treatment prior to quenching is not itself responsible for the observed change in the lamellar thickness. The slowly cooled control samples did not show an increase in lamellar thickness. A small decrease was in fact observed, and in this case the changes could well be due to annealing of the samples.

Finally, the data of Table 5.4 shows that the lamellar thickness is independent of the time that the polyethylene samples were maintained at 70°C. If the annealing mechanism were operating at this temperature it would have caused a progressive decrease with time of the L.A. mode. The data obtained therefore provides further evidence against the suggested annealing explanation.

These initial studies suggest that the observed effect may well be thermodynamically controlled. Prior to this work it had been suggested that the trans to gauche ratio determines the lamellar thickness in polyethylene quenched from the melt (93). However, it was not possible to test this hypothesis directly as no reliable method is available for estimating the trans to gauche ratio in polyethylene.

The work of Rafi-Ahmed and Charlesby provides some support for the view that lamellar thickness may vary at temperatures below the melting point (116). These authors used the technique of pulsed N.M.R. to observe changes in polyethylene and found a steady increase in the crystallinity as the temperature was lowered beyond the melting point. It was also pointed out that a good correlation exists between crystallinity data obtained by pulsed N.M.R. and by density measurements.

REFERENCES

(1) R.E. Robertson, J. Phys. Chem. 69, 1575, (1965)

(2) M. Kurata, W.H. Stockmayer, Fortschr. Hochpolym. Forsch., 3,196, (1963).

(3) S. Masuoka, J. Appl. Phys. 32, 2334, (1961)

(4) R.L. Miller, L.E. Nielsen, J. Polym, Sci., 55, 643 (1961)

(5) S. Onogi, et. al., J. Polym. Sci., 58, 1, (1962)

(6) W.H. Starkweather, R.E. Moyniham, J. Polym. Sci., 22, 363, (1965)

(7) V.A. Kargin, J. Colloid, U.S.S.R. English translation, 19, 141,(1957

(8) E.W. Fischer, J. Macromol, Sci-Phys., B12,(1), 41, (1976)

(9) G.S.Y. Yeh, P.H. Geil, J. Macromol Sci., B1, 235, 251 (1967)

(10) G.S.Y. Yeh, J. Macromol Sci-Phys., 136(3), 465, (1972)

(11) Th. G. Schoon, Proc. Internat. Rubber Conf. B1, 235, 251, (1967)

(12) P.J. Harget, A. Siegmann, J. Appl. Phys., 43, 4357, (1972)

(13) J.R. Katz, Z. Phy. Chem., A125, 321, (1927)

(14) W. Pechhold, Die Angervandte Makromol, Chemie, 22, 3, (1972)

(15) P.J. Flory, Statistical Mechanics of Chain Molecules, Wiley, New York, (1969)

(16) D. McIntyre, et. al., J. Phys. Chem., 66, 1932, (1962)

(17) K. Hermann, O. Gerngoss, Kantschuk, 8, 181, (1932)

(18) W.H.D. Bryant, J. Polym. Sci., 2, 547, (1947)

(19) C.W. Bunn, T.C. Allcock, Trans. Farad. Soc., 41, 317, (1945)

(20) A. Keller, J. Polym. Sci., 17, 291, (1955)

(21) A. Keller, Phil, Mag., 2, 171, (1957)

(22) E.W. Fischer, Z. Naturforsch, 129, 753, (1957)

(23) P.H. Till, J. Polym. Sci., 24, 301, (1957)

(24) B.G. Ranby, F.F. Morehead, N.M. Walters, J. Polym Sci., 34, 349, (1960)

(25) P.H. Geil, N.K.J. Symons, R.G. Scott, J. Appl. Phys. 30, 1516, (1959)

(26) P.H. Geil, J. Polym. Sci., 44, 449, (1960)

(27) Y. Yamashita, J. Polym. Sci., A3, 81, (1965)

(28) F.J. Padden, H.D. Keith, J. Appl. Phys., 36, 2987, (1965)

(29) P.H. Geil, J. Polym.Sci., 51, 510, (1961)

(30) R.P. Palmer, A.J. Cobbold, Makromol, Chem, 74, 174, (1964)

(31) A. Keller, S. Sawada, Makromol, Chem, 74, 190, (1964)

(32) Y. Yamashita, J. Polym, Sci., 59, 539, (1962)

(33) P.J. Hendra, Chapter 6, in Structural Studies of Macromolecules by Spectroscopic Methods, ed. K.J. Ivin, Wiley, (1976)

(34) A. Keller, A. O'Connor, Disc. Faraday Soc., 25, 114, (1958)

(35) D.H. Reneker, J. Polym. Sci., 59, 532, (1962)

(36) A. Keller, D.J. Priest, J. Polym. Sci., 138, 13, (1970)

(37) P. Dreyfuss, A. Keller, J. Polym Sci., 138, 253, (1970)

(38) P. Dreyfuss, A. Keller, J. Macromol, Sci., B, 4, 811, (1970)

(39) F.W. Billmeyer, Textbook of Polymer Science, Wiley, New York (1971)

(40) E.W. Fischer, R. Lorentz, Kolliod-Z.Z. Polymers 189, 97, (1963)

(41) J.B. Jackson, P.J. Flory, R. Chiang, Trans. Faraday. Soc, 59, 1906, (1963)

(42) T. Kawai, Makromol Chem., 90, 288, (1966)

(43) A. Keller, Kolliod-Zeits. Polymers, Bd, 231(1), 286 (1969)

(44) R.P. Palmer, A. Cobbold, Makromol Chem. 74, 174, (1964)

(45) A. Keller, Rept. Progr. Phys., 31, (11), 623, (1968)

(46) F.C. Frank, M. Tosi, Growth and Perfection of Crystals, Proc. Int. Conf., Interscience, New York, (1958)

(47) A. Peterlin, E.W. Fischer, Z. Phys., 159, 272, (1960)

(48) J.I. Lauritzen, I.D. Hoffman, J. Res. Nat. Bur. Stand, A, 64, 73, (1960)

(49) F.P. Price, J, Chem, Phys., 35, 1884, (1961)

(50) F.C. Frank, M. Tosi, Proc. Roy. Soc. A, 623, 323, (1961)

(51) J.I. Lauritzen, A.E. Passaglia, J. Res. Nat. Bur. Stand, A, 71, 261, (1967)

(52) T. Kawai, A. Keller, Phil. Mag., 8, 1203, (1965)

(53) D. Aitken, M. Glotin, P.J. Hendra, H. Jobic, E. Marsden, J. Polym. Sci. Polym. Lett., 14, 619 (1976)

(54) P.J. Hendra, E.R. Scerri, M.E.A. Cudby , H. Willis, (Submitted to Polymer).

(55) J. Schelten, et. al., Polymer 15, 682, (1974)

(56) J. Schelten, et. al., Colloid and Polymer Sci. 252, 749, (1974)

(57) D.G.H. Ballard, G.D. Wignall, G. Longman, Polymer Preprints 18(2), 167, (1977)

(58) P.H. Lindmeyer, V.P. Holland, J. Appl. Phys., 35, 55, (1964)

(59) J.D. Hoffman, et. al., J. Res. N.B.S. 79A, 671, (1975)

(60) P.E. Rouse, J. Chem. Phys., 21, 1272, (1953)

(61) P.J. Flory, J. Am. Chem Soc., 84, 2857, (1962)

(62) E.W. Fischer, G. Schmidt, Angew Chem. 74, 551, (1962)

(63) P.J. Flory, and D.Y. Yoon, Nature, 272, 226, (1978)

(64) G. Zerbi, L. Piseri, F. Cabassi, J. Molec. Phys. 22, 241, (1971)

(65) H. Jobic, M. Phil, Thesis, Southampton University, (1975)

(66) Urch, Orbitals and Symmetry, Penguin, (1970)

(67) G.H. Hertzberg, Molecular Spectra and Molecular Structure 2nd Ed., D. Van Nostrand Co., (1950)

(68) S. Mizushima, T. Simanonchi, J. Chem. Phys., 47, 3605, (1967)

(69) W.L. Peticolas, G.W. Hibler, J.L. Lippert, A. Peterlin, A. Olf, Appl. Phys., Lett., 18, 87, (1971)

(70) H.G. Olf, A. Peterlin, W.L. Peticolas, J. Polym. Sci., 12, D359, (1974)

(71) M.J. Folkes, A. Keller, J. Steiny, G.V. Fraser, P.J. Hendra, Kolloid Z. uZ Polymers, 253, 354, (1975)

(72) G.V. Fraser, Indian J. Pure & App. Phys., 16, 344 (1978)

(73) G. V. Fraser, Polymer, 19, 857, (1978)

(74) D.J. Cutler, (unpublished work, Southampton University).

(75) B. Fanconi, J. Crissman, J. Polym. Sci. Polym. Lett. Ed., 13, 421, (1975)

(76) L. Lippert, W.L. Peticolas, Biochem, Biophys. Acts., 282, 8, (1972)

(77) G.R. Stroebl, R. Eckel, J. Polym. Sci., Phys. Ed., 14, 913, (1976)

(78) A. Peterlin, G. Meinel, J. Poly. Sci., 83, 1059

(79) D.J. Preist, J. Poly. Sci., A-2, 1777)1971)

(80) P.J. Hendra, E.P. Marsden, et. al. Die Makromol, Chem., 176, 2443 (1975)

(81) A. Keller, Y. Ugadawa, J. Poly. Sci., A-2, 9, 1793 (1971)

(82) A. Keller, Y. Ugadawa, J. Poly. Sci. A2, 437, (1971)

(83) D. Dreyfuss, G.V. Fraser, E.J. George, A. Keller, paper Presented to Vth Int. Conf. on Raman Spectroscopy, Freiburg, September, (1976)

(84) A. Hartley, Y.K. Leung, C. Booth, J. McMahon, I.W. Shepherd, Polymer, 18, 336, (1977)

(85) S.L. Hau, S. Krimm, S. Krause, J.S.Y. Yen, J. Poly. Sci., Polymer Lett. Ed., 14, 195, (1976)

(86) J.F. Rabolt, B. Fanconi, J. Poly. Sci., Poly. Lett. Edn., 15, 121, (1977)

(87) I. Sakurada, K. Kaji, J. Poly. Sci., C, 31, 57, (1970)

(88) L. Piseri, C. Zerbi, J. Chem. Phys., 48, 3561, (1968)

(89) J. White, in "Structural Studies of Macromolecules by Spectroscopic Methods" ed. K.J. Ivin, New York, (1976)

(90) T.R. Gilson, P.J. Hendra, Laser Raman Spectroscopy, Wiley, London, (1970)

(91) L. Bragg, The development of X-ray Analysis, Bell & Son, 1975

(92) J.W. Turley, X-ray Diffraction Patterns of Polymers, Dow Chemical Co., 1965

(93) A. Guinier, G. Fournet, Small-Angle Scattering of X-Rays, John Wiley, New York, (1955)

(94) P.J. Hendra, E.P. Marsden, M.E.A. Cudby, H.A. Willis, Die Makromol,Chemie, 176, 2443, (1975)

(95) D. Aitken, D. Cutler, M. Glotin, P.J. Hendra, H.P. Jobic, E.P. Marsden, M.E.A. Cudby and H.A. Willis (submitted to Polymer)

(96) A. Hartley, Y.K. Leung, C. Booth, I.W. Shepherd, Polymer, Vol. 17, 355 (1978)

(97) P.J. Hendra, H.P. Jobic, K. Holland-Moritz. J. Poly. Sci., Poly-Lett. End., 13, 365 (1975)

(98) H.P. Jobic, M. Phil. Thesis, Southampton University (1975)

(99) M. Davis, Infra-Red Spectroscopy, & Molecular Structure, Elvesier (1963)

(100) M. Glotin, PhD Thesis, Southampton University, (1978)

(101) G. Zerbi, P.J. Hendra, J. Molec. Spec., 27, 17, (1968)

(102) J.L. Koneig, A.C. Angood, J. Poly. Sci., Part A2, 8, 1787 (1970)

(103) H. Matsuura, T. Miyazawa, J. Poly. Sci., Part A2, 7, 1735, (1969)

(104) H. Willis chapter in Molecular Spectroscopy eds. Bevan and Johnson, Heywood, (1961)

(105) Identification and Analysis of Plastics, Haslam, Willis and Squirell, Illife Books (1971)

(106) Discussions with A. Charlesby, R. Folland, P. Fydelor, M.E.A. Cudby, H.A. Willis

(107) A. Charlesby, R. Folland, J.H. Stevens, Proc. R. Soc. Lond. A., 355, 189 (1977)

(108) A. Charlesby, Proc. Phys. Soc., 57, 496, (1945)

(109) T. Kawai, A. Keller, A. Charlesby, M.G. Ormerod, Phil. Mag., 10, 779 (1964)

(110) Y. De. Zarauz, C.R. Acad. Sc. Paris, 1348 (1959)

(111) J. Rault, C.R. Acad. Sc. Paris, 385B, 321, (1977)

(112) A. Peterlin, communication with P.J. Hendra.

(113) L.G.R. Treloar, Introduction to Polymer Science, Wykenham Publications (1970)

(114) J.M.G. Cowie, in Polymers: Chemistry and Physics of Modern Materials, Ed. K. Stead, International Textbooks (1973)

(115) Private communication with Dr. P.J. Hendra.

(116) A. Charlesby, S. Rafi-Ahmed, Eur. Poly. J., 11, 91, (1975)

Appendix removed

Hendra P. J., Scerri E. R., Cudby M. E. A., and Willis H. A. (1979) 'The Structure of Crystalline Polymers Produced by Rapid Cooling of their Melts II Polyoxymethlene', *Polymer*, Vol 20 (12).

Available at: DOI: 10.1016/0032-3861(79)90011-9.

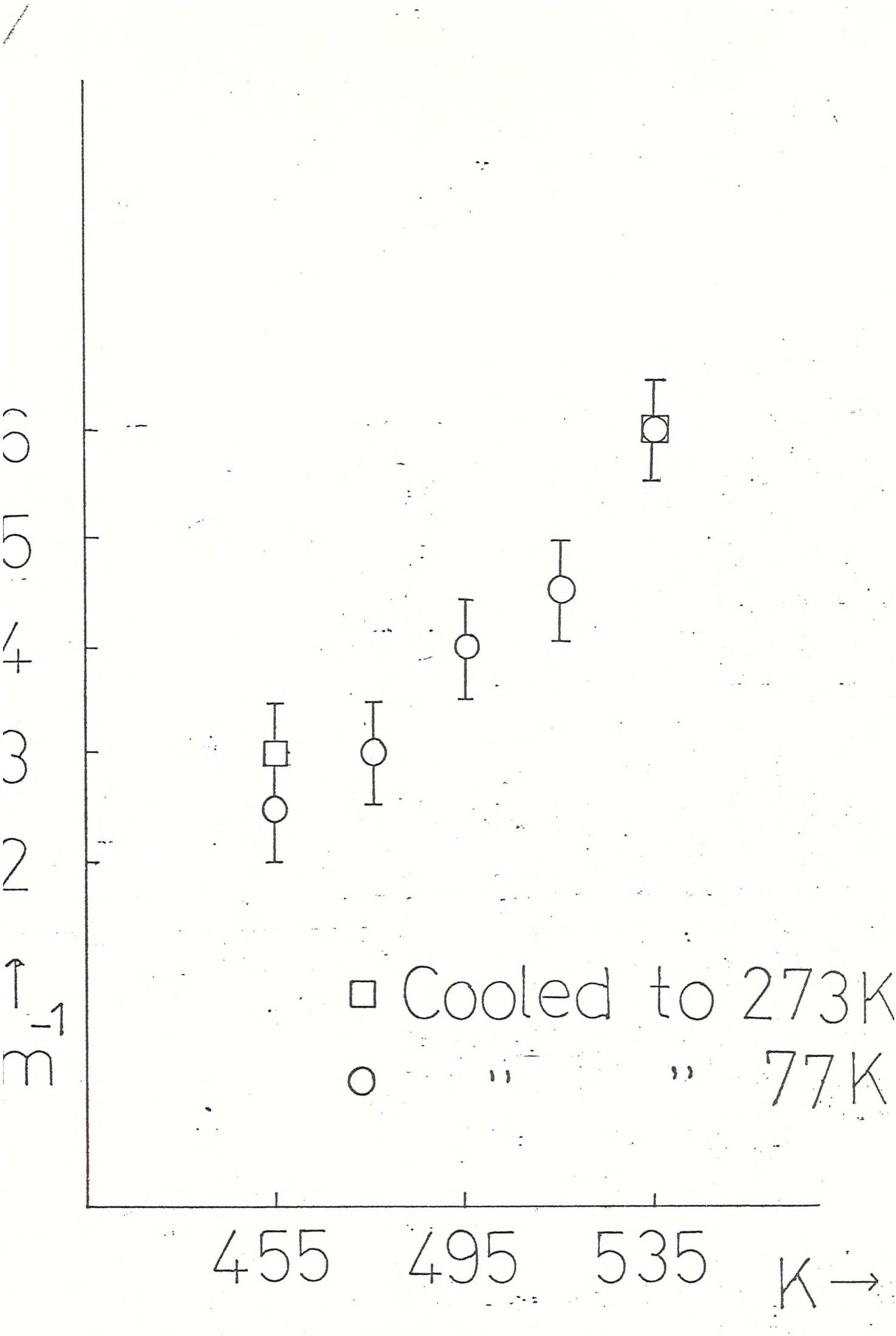
5
4
3
2
m^{-1}
□ Cooled to 273K
○ " " 77K
455
495
535
K →

TABLE I

Melt Temp. K	L.A. mode cm^{-1}	$l_c / 2l_f + l_c$
455	12.5 ± 0.5	0.64 ± 0.1
495	14.0 ± 0.5	0.68 ± 0.1
535	16.0 ± 0.5	0.65 ± 0.1

TABLE 3.

Melt Temp. of film sample K	L.A. mode cm^{-1}	Number & size of spherulites
458	14 ± 0.5	Large number, small.
523	16 ± 0.5	Small number, large.
Re-melted at 458	14 ± 0.5	~~Large~~ Small number large ~~small~~.